Supporting Information

Atmospheric oxidation pathways of $CF_3CH_2CFCl_2$ (HCFC-234fb) with OH-radicals and Cl-atoms: insights into the mechanism, thermodynamics, and kinetics

Rabu Ranjan Changmai, Samsung Raja Daimari, Anand Kumar Yadav, and Manabendra Sarma*

Department of Chemistry, IIT Guwahati, Guwahati -781039, Assam, India

E-mail: msarma@iitg.ac.in

The Supporting Information contains the vibrational frequencies of the species to confirm the transition states at M06-2X and MP2 level of theories involved in the reaction of DTP with OH-radical and Cl-atom. The Supporting Information also contains the absolute energies, Gibbs free energies, and enthalpies of all the species involved in the reactions. The IRC comparison plots have been provided for all the reaction channels. The Supporting Information also contains all the equilibrium constants, unimolecular rate coefficients and overall rate coefficients for all the reaction channels in the temperature range 200-400 K.

Table of Contents

Table S13: Intrinsic reaction coordinate data (IRC) for the abstraction of Cl-atom of DTP with Cl-atom calculated at the **MP2/cc-pVTZ level of theory (R4B).**

Figure S4: Intrinsic reaction coordinate (IRC) plots for the R1B-R2B and R3B-R4B at the **MP2/cc-pVTZ level of theory**.

Table S14: Single point energy calculated at the **CCSD (T)/aug-cc-pVTZ//MP2/cc-pVTZ level of theory** of all the species involved in the reaction (A).

Table S15: Single point energy calculated at the **CCSD (T)/aug-cc-pVTZ//MP2/cc-pVTZ level of theory** of all the species involved in the reaction (B).

Table S16: Relative energies of the species involved in the reaction of DTP with $^{\bullet}$OH and Cl at the **CCSD(T)/aug-cc-pVTZ//MP2/cc-pVTZ** level of theory. Energies are in kcal/mol.

Table S17: *T1*-diagnostic and **spin-contamination values, $<S^2>$** for all the stationary points involved in the reaction of DTP with OH-radical calculated at the **CCSD(T)/aug-cc-pVTZ level of theory.**

Table S18: *T1*-diagnostic and **spin-contamination values, $<S^2>$** for all the stationary points involved in the reaction of DTP with Cl-atom calculated at the **CCSD(T)/aug-cc-pVTZ level of theory.**

Table S19: Calculated Equilibrium constant (K_{eq}), unimolecular rate coefficient (k_{uni}) and overall rate coefficients (k_{1A}, k_{2A}, k_{3A}, k_{4A}) for the reaction channel **R1A, R2A, R3A**, and **R4A** in the 200-400 K temperature range at the **M06-2X level of theory**. Units of rate coefficients are in cm^3 $molecule^{-1}$ s^{-1}.

Table S20: Calculated overall rate coefficients for the reaction of $CCl_2FCH_2CF_3$ with OH-radical in the 200-400 K temperature range at the M06-2X level of theory. Units are in cm^3 $molecule^{-1}$ s^{-1}.

Table S21: Calculated Equilibrium constant (K_{eq}), unimolecular rate coefficient (k_{uni}) and overall rate coefficients (k_{1B}, k_{2B}, k_{3B}, k_{4B}) for the reaction channel **R1B, R2B, R3B**, and **R4B** in the 200-400 K temperature range at the M06-2X level of theory. Units of rate coefficients are in cm^3 $molecule^{-1}$ s^{-1}.

Table S22: Calculated overall rate coefficients for the reaction of $CCl_2FCH_2CF_3$ with Cl-atom in the 200-400 K temperature range at the **M06-2X level of theory**. Units are in cm^3 $molecule^{-1}$ s^{-1}.

Notes 2: **Eckart Unsymmetrical Potential Barrier.**

Table S23: Vibrational frequencies which are treated as hindered rotors for the species involved in the dominant reaction channels (R1A, R2A, R1B, and R2B) calculated at the M06-2X/cc-pVTZ level of theory. Units are in cm^{-1}.

Notes 3: Hindered Rotor (HR) Approximation.

Table S24: Calculated Eckart tunneling contributions (Γ_x, x = OH-1A, OH-2A, OH-3A, OH-4A) for all the four reaction channels (R1A, R2A, R3A, R4A) involved in the reaction of DTP with $^{\bullet}OH$ in the temperature range of 200-400 K using Eyringpy Program code at the **M06-2X level of theory**.

Table S25: Calculated Eckart tunneling contributions (Γx, x = Cl-1B, Cl-2B, Cl-3B, Cl-4B) for all the four reaction channels (R1B, R2B, R3B, R4B) involved in the reaction of DTP with Cl-atom in the temperature range of 200-400 K using Eyringpy Program code at the **M06-2X level of theory**.

Table S26: Branching ratio for the reaction of DTP with OH-radical in the 200-400 K temperature range.

Table S27: Branching ratio for the reaction of DTP with Cl-atom in the 200-400 K temperature range.

Notes 4: Radiative Efficiency Calculations.

Table S28: Frequencies and intensities of $CF_3CH_2CFCl_2$ calculated at the **M06-2X level of theory**.

Table S1: Energy of the $CF_3CH_2CFCl_2$ (DTP) molecule for every 10° rotation of the C-C bond to get the optimized conformers.

Scan (°)	Energy (Hartree)
0	-1433.6211
10	-1433.6207
20	-1433.6195
30	-1433.6175
40	-1433.6153
50	-1433.6137
60	-1433.6134
70	-1433.6145
80	-1433.6165
90	-1433.6185
100	-1433.6198
110	-1433.6201
120	-1433.6201
130	-1433.6198
140	-1433.6187
150	-1433.6167
160	-1433.6147
170	-1433.6134
180	-1433.6136
190	-1433.6151
200	-1433.6173
210	-1433.6194
220	-1433.6207
230	-1433.6211
240	-1433.6210
250	-1433.6206
260	-1433.6197
270	-1433.6182
280	-1433.6166
290	-1433.6155
300	-1433.6156
310	-1433.6168
320	-1433.6184
330	-1433.6198
340	-1433.6206
350	-1433.6209
360	-1433.6211

Notes 1: Molecular Electrostatic Potential Surface Studies.

The molecular electrostatic potential (MESP) studies provide a visual way to understand the various properties of the molecule. In the current work, MESP is used to predict the reactive sites of the molecule. The electrostatic potential maps of $CF_3CH_2CFCl_2$, OH-radical, and Cl-atom are shown in Fig. S1. The blue color indicates positive potential and red color indicates negative potential. In addition, the darker the color, greater is the magnitude of the potential. From Figure S1, we see that fluorine (F) atom is much more electronegative compared to the hydrogen (H) and chlorine (Cl)-atom. This means that breaking the C-F bind would require high energy. As a result, OH-radical cannot abstract the F-atoms. Similarly, the Cl-atom also cannot abstract the F-atom, which would necessitate extremely high energy to rupture the bonds already present.

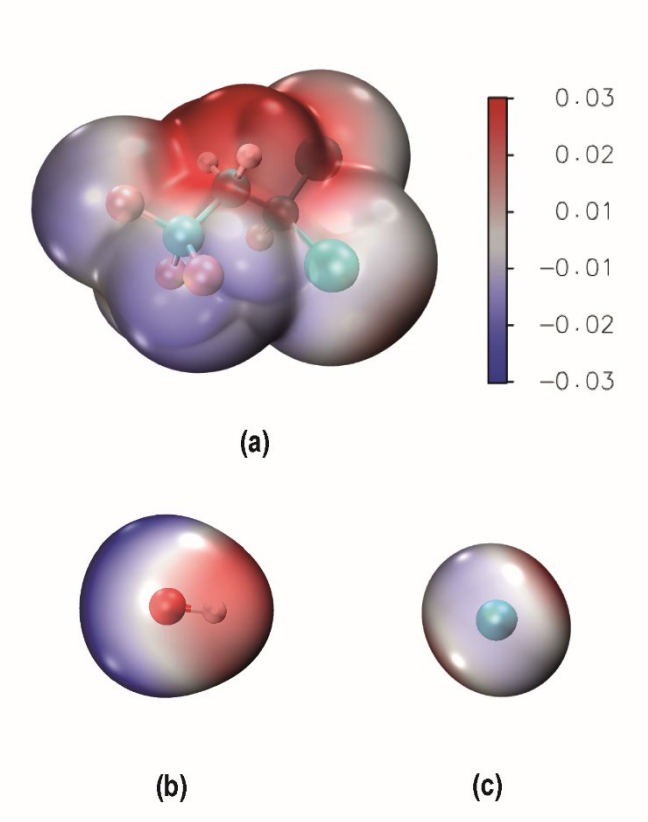

Figure S1: Computed molecular electrostatic potential maps for (a) DTP, (b) OH-radical, and (c) Cl-atom at the MP2/cc-pVTZ theoretical level. The color represents electron density distribution: Blue represents highest electron density site and red represents low electron density site. The isovalue of the surface is 0.02.

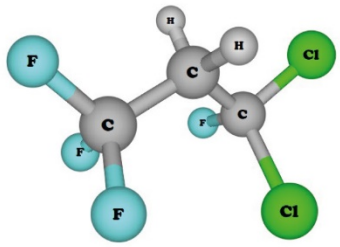

(1) DTP

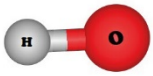

(2) OH

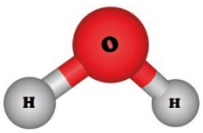

(3) Water

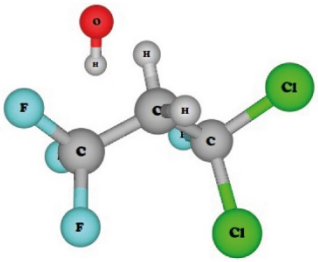

(4) CR1A

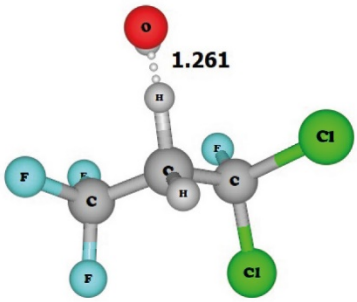

(5) TS1A

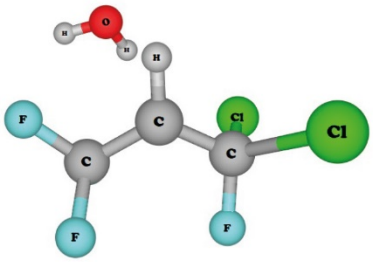

(6) PC1A

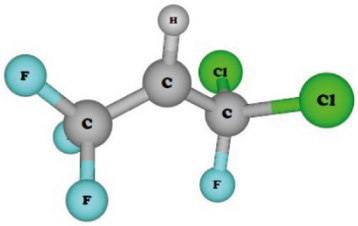

(7) P1A

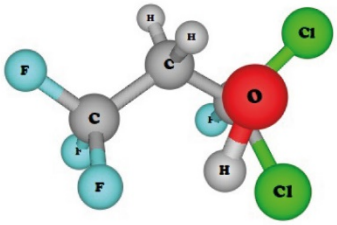

(8) CR2A

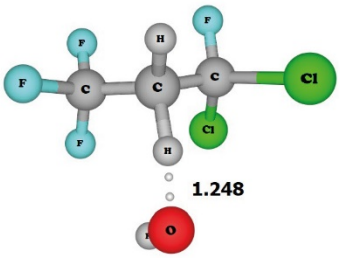

(9) TS2A

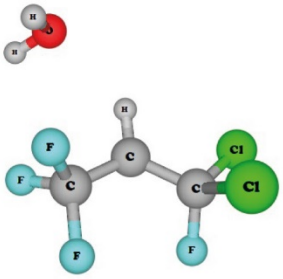

(10) PC2A

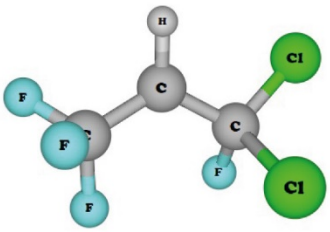

(11) P2A

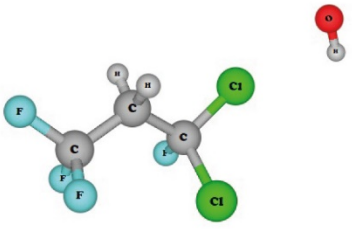

(12) CR3A

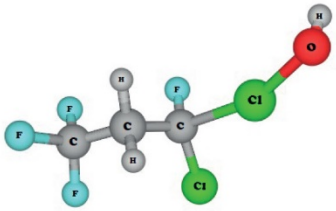

(13) TS3A

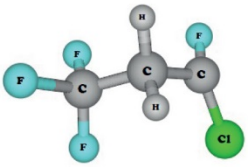

(14) PC3A

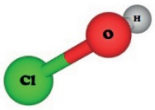

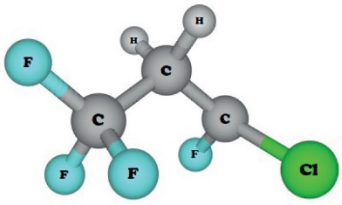

(15) P3A

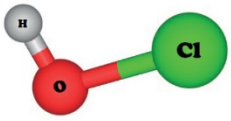

(16) HOCl

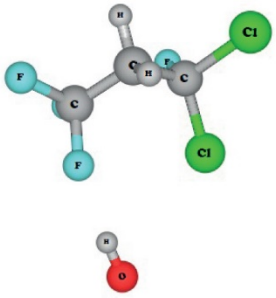

(17) CR4A

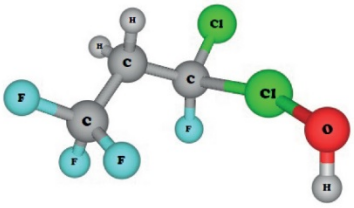

(18) TS4A

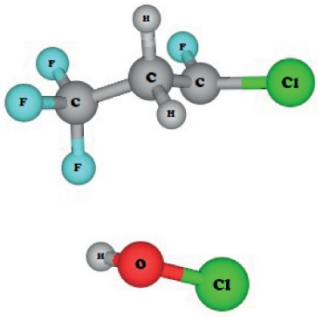

(19) PC4A

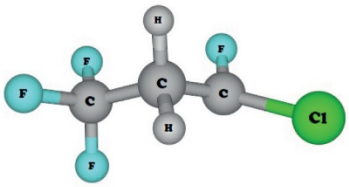

(20) P4A

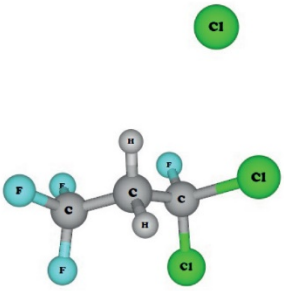

(21) CR1B

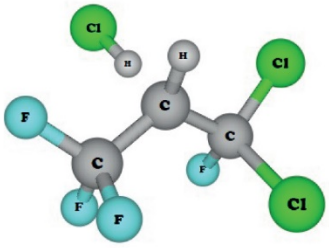

(22) TS1B

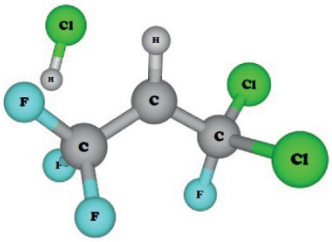

(23) PC1B

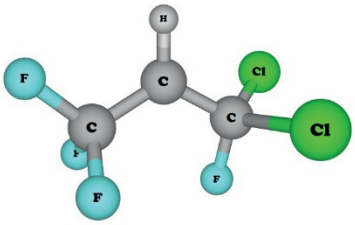

(24) P1B

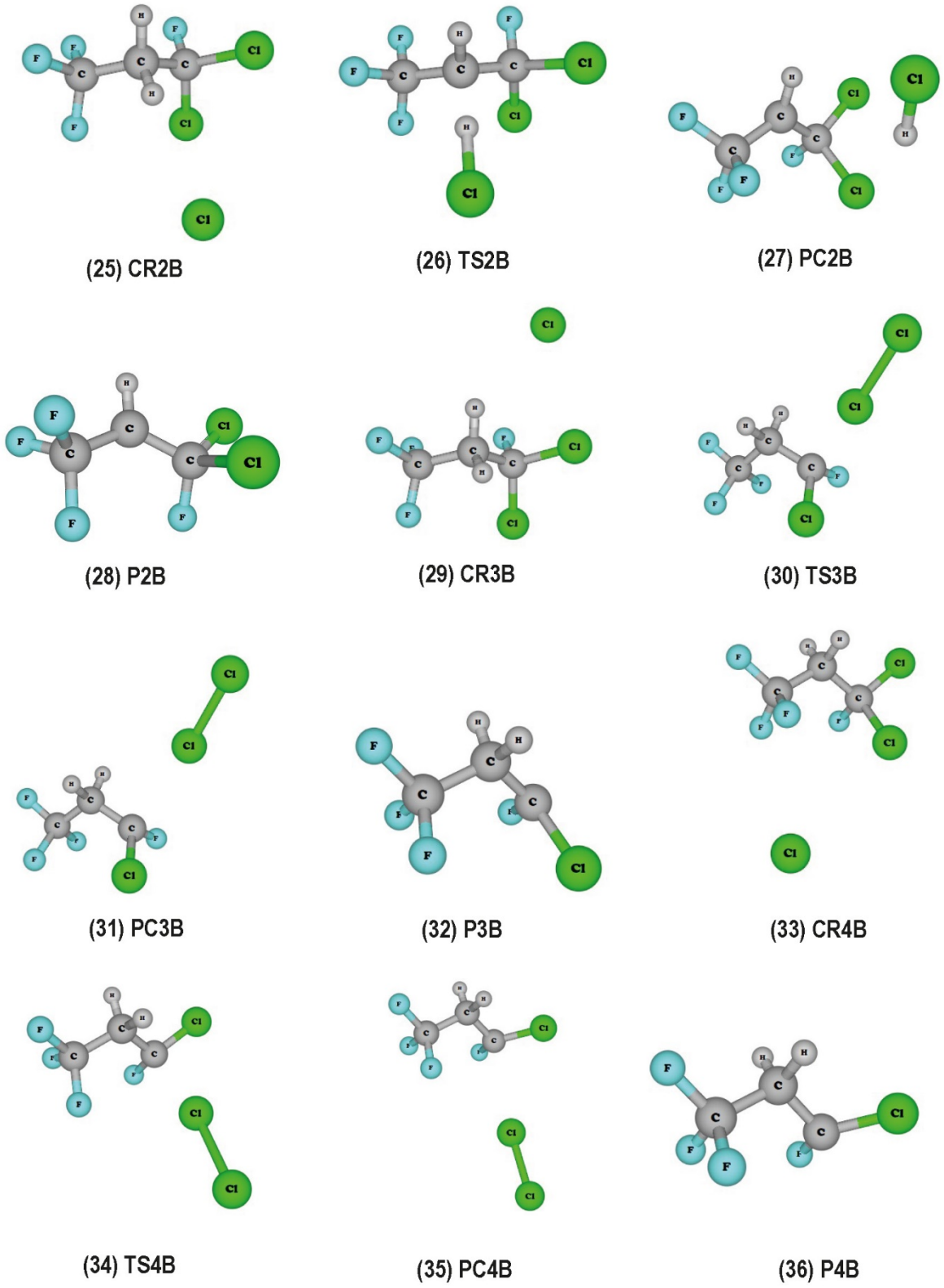

Figure S2: Optimized structures of all the species involved in the oxidation of DTP by OH-radical and Cl-atom at the **MP2/cc-pVTZ** level of theory.

Table S2: Vibrational frequencies of the reactants, pre-reactive complexes, transition states, product complexes, and products for the reaction of CFP and OH-radicals calculated at the **M06-2X/cc-pVTZ level of theory.** All the frequency values are in cm^{-1}.

Reactant	OH	CR1A	TS1A	PC1A	P1A	H_2O	CR2A	TS2A
30.37	3773.96	22.42	-1599.31	25.68	27.8	1626.63	28.92	-1668.76
123.34		66.84	17.20	27.45	41.16	3877.31	62.15	33.68
147.63		74.55	71.58	93.20	137.29	3979.36	85.2	66.95
230.95		113.64	87.88	108.48	215.49		116.9	87.38
243.14		141.49	135.51	124.41	227.46		151.83	138.53
306.12		158.08	156.93	136.05	310.95		157.3	148.01
328.53		231.59	167.94	151.32	327.71		232.94	165.54
387.17		238.22	229.81	226.62	330.24		246.12	228.73
408.13		247.43	234.7	228.93	387.17		273.78	246.28
467.92		307.18	307.07	271.28	459.7		306.8	306.3
539.21		324.51	325.05	290.89	487.6		330.01	325.75
550.41		330.01	337.21	304.86	544.86		341.75	346.7
655.52		389.7	394.22	324.84	601.32		390.73	391.53
702.65		415.06	468.34	332.76	656.41		417.71	469.63
845.13		470.4	539.75	383.51	769.92		468.96	531.95
896.61		540.46	546.57	461.27	825.14		538.85	550.51
934.92		551.26	656.25	487.67	891.37		550.94	655.68
1039.23		655.85	692.23	547.38	1022.8		657.63	674.48
1179.63		700.98	770.11	601.34	1209.7		696.04	757.09
1217.1		847.33	836.09	660.83	1223.48		847.67	800.52
1240.74		892.84	862.48	752.36	1239.77		896.37	850.11
1317.47		935.43	892.08	838.13	1298.05		932.7	911.98
1345.92		1031.59	977.28	889.15	1426.15		1043.1	974.36
1418.79		1175.23	1040.49	1025.72	3273.9		1173.73	1045.19
1458.48		1222.39	1111.95	1187.16			1223.3	1148.08
3113.06		1231.37	1212.21	1223.36			1237.73	1173.62
3176.06		1305.23	1230.15	1232.89			1312.9	1228.53
		1345.69	1272.5	1291.44			1347.83	1274.28
		1424.61	1309.34	1422.97			1424.81	1301.25
		1455.75	1403.63	1617.87			1461.5	1401.03
		3115.52	1456.08	3286.94			3114.07	1443.92
		3177.96	3173.73	3859.15			3180.4	3152.61
		3761.52	3771.74	3959.79			3757.88	3775.94

PC2A	P2A	CR3A	TS3A	PC3A	P3A	HOCl	CR4A	TS4A
25.62	27.17	27.04	-364.13	23.12	30.58	806.01	21.81	-348.29
49.94	53.59	62.11	24.73	29.93	90.58	1284.91	65.38	30.4
64.05	145.2	68.72	40.43	35.89	126.36	3849.46	82.14	57.47
73.28	223.6	119.47	79.17	65.5	262.78		119.59	84.1
96.63	244.16	139.49	88.39	81.64	304.76		144.43	114.45
129.85	294.22	147.98	121.96	86	391.71		161.51	122.36
154.43	312.68	224.5	145.49	92.22	412.98		230.86	153.33
217.5	326.54	233.2	168.02	115.11	486.92		245.13	185.4
229.9	390.19	244.09	213	129.98	542.61		272.63	202.03
254.15	464.43	306.4	278.14	264.18	548.82		312.14	272.17
261.11	509.06	328.53	287.08	307.03	670.4		327.21	294.92
301.5	542.8	357.02	324.07	395.7	736.62		330.68	323.27
324.45	621.15	391.74	402.19	418.5	861.18		381.59	376.99
376.87	665.42	412.8	439.2	497.9	931.84		420.86	439.35
402.29	731.85	468.48	536.95	543.29	1066.94		466.44	519.48
465.2	852.57	539.79	546.31	550.63	1187.96		545.96	545.45
527.78	892.55	551.35	576.51	676.73	1224.85		547.26	566.59
543.37	1034.5	655.81	689.46	737.79	1286.07		650.78	659.79
634.23	1194.13	705.24	738.36	778.9	1321.89		708.78	813.51
664.56	1213.05	843.91	870.65	862.95	1347.7		840.95	875.56
731.06	1231.26	895.27	932.67	931.98	1389.5		881.25	935.09
850.16	1326.91	934.07	1058.62	1069.48	1450.76		957.79	1045.24
890.63	1419.9	1034.31	1114.5	1189.51	3101.19		1034.13	1133.82
1035.61	3260.71	1178.19	1187.77	1226.96	3163.29		1184.22	1168.87
1174.54		1221.84	1222.62	1275.5			1216.65	1223.37
1198.48		1232.5	1280.47	1286.87			1241.22	1277.81
1231.34		1316.36	1314.16	1320.98			1309.8	1317.75
1330.95		1346.42	1341.94	1347.64			1344.27	1335.2
1420.62		1422.78	1397.26	1392.24			1426.48	1416.66
1630.06		1464.34	1451.36	1449.89			1461.74	1457.01
3252.84		3113.83	3112.3	3102.29			3116.24	3084.14
3861.29		3176.48	3173.65	3163.36			3180.47	3158.02
3958.16		3762.49	3837.2	3845.86			3761.81	3835.16

PC4A	P4A	CR1B	TS1B	PC1B	P1B	HCl	CR2B	TS2B
31.82	27.67	16.86	-946.43	22.43	28.52	2995.06	35.43	-1010.56
13.4	80.45	35.08	21.64	27.05	54		38.13	30.83
43.43	140.85	52.2	45.56	39.01	144.59		66.34	41.59
56.37	262.79	98.84	69.41	70.44	223.13		106.96	68.9
67.43	311.28	126.14	106.55	78	243.62		135.36	100.82
74.29	362.68	148.43	152.85	148.06	295.04		149.29	144.59
106.21	416	234.99	218.03	185.68	312.75		232.54	224.85
123.88	437.43	244.75	227.89	221.6	325.58		244.09	240.59
147.45	544.04	306.13	301.28	240.04	389.9		307.04	302.37
259.7	551.25	328.36	321.3	278.47	464.76		329.87	315.18
314.5	656.3	385.26	330.72	301.86	509.2		389.47	356.25
365.76	803.25	407.07	392.91	322.55	542.92		414.38	389.56
419.04	873.64	465.43	467.42	334.09	621.98		467.73	439.76
436.95	923.47	539.33	491.16	392.31	664.69		538.68	481.46
545.04	1064.65	551.07	546.38	464.54	733.01		550.56	533.69
553.97	1167.39	653.96	547.68	515.55	850.41		655.73	553.26
660.31	1233.45	702.92	655.88	543.21	891.74		690.17	663.99
791.28	1282.2	833.67	715.39	629.4	1035.14		847.29	695.03
823.58	1327.47	894.64	802.04	663.68	1194.15		894.92	768.75
876.88	1338.95	934.11	841.37	736.57	1214.27		936.55	785.32
927.44	1406.9	1042.49	851.99	844.89	1231.51		1038.96	854.36
1060.07	1452.38	1182.96	895.24	889.11	1327.42		1176.53	917.29
1162.88	3060.74	1222.24	1012.94	1033.71	1420.65		1221.16	1079.55
1229.04	3166.26	1246.68	1104.04	1188.42	3261		1244.67	1098.6
1278.35		1318.02	1225.17	1202.32			1315.7	1166.43
1284.64		1347.98	1233.58	1238.52			1346.27	1224.35
1325.02		1421.47	1244.65	1332.37			1421.95	1258.16
1337.24		1458.14	1322.14	1420.28			1459.59	1306.26
1415.25		3108.05	1399.36	2974.03			3113.4	1397.48
1454.99		3174.43	3198.38	3258.63			3177.46	3182.69
3057.34								
3147.14								
3847.92								

PC2B	P2B	CR3B	TS3B	PC3B	P3B	Cl_2	CR4B	TS4B
35.96	25.76	25.38	-268.6	22.11	29.44	578.37	37.12	-295.09
38.09	52	34.33	25.1	24.96	90.29		38.58	34.34
56.11	145.09	53.34	37.68	38.15	125.59		66.31	39.3
68.56	223.22	101.22	54.04	63.24	262.64		105.02	63.85
97.57	244.02	127.63	97.58	74.61	304.28		136.09	94.27
140.57	293.07	147.33	112.34	80.63	391.02		151.12	137.36
195.76	311.13	235.33	137.6	93.09	412.6		232.46	152.5
229.4	326.52	244.96	175.04	130.89	486.84		243.85	172.78
243.22	389.59	306.2	229.58	264.66	542.5		306.98	239.13
261.07	464.75	328.06	273	307.02	548.79		329.59	267.6
305.92	508.06	386.4	313.99	395.34	670.37		389.14	318.71
324.16	542.99	409.73	400.92	419.78	736.54		413.41	368.13
345.83	620.1	464.95	435.56	502.5	861.17		467.84	440.65
389.42	664.68	539.28	522.14	521.82	931.34		538.47	466.7
466.73	731.13	551.08	544.92	543.17	1066.19		550.92	545.08
495.12	850.68	654.04	557.74	551.18	1187.78		655.72	556.44
541.62	892.13	703.42	689.11	679.83	1224.78		691.55	662.64
607.92	1035.11	832.98	741.2	738.75	1285.99		847.93	820.25
669.08	1193.78	894.48	869.62	863.56	1321.9		895.17	878.01
720.27	1214.19	934.04	935.4	932.23	1346.98		935.3	931.32
861.64	1231.55	1043.08	1068.87	1069.14	1388.92		1038.35	1056.49
901.38	1328.21	1182.1	1195.27	1190.83	1450.17		1175.75	1166.05
1043.13	1421.01	1222.79	1228.53	1227.79	3101.29		1220.99	1227.8
1170.72	3258.32	1246.61	1289.55	1287.98	3163.47		1243.45	1291.61
1200.62		1317.5	1317.93	1320.62			1315.73	1324.42
1231.81		1347.44	1345.77	1346.78			1344.94	1340.97
1321.14		1421.34	1391.08	1389.71			1420.51	1416.15
1420.43		1459.99	1451.36	1449.42			1458.87	1454.15
2964.21		3112	3112.63	3102.1			3112.3	3078.12
3273.73		3176.17	3175.22	3163.71			3174.67	3152.49

PC4B	P4B
18.87	31.17
28.53	80.62
42.99	140.9
61.73	262.38
64	311.33
69.25	362.71
105.71	416.81
145.89	438.07
259.65	543.45
313.66	551.24
366.78	656.45
423.55	804
437.09	873.79
545.46	924.26
553.59	1064.4
555.3	1167.09
660.28	1233.11
821.77	1282.71
877.4	1327.63
928.66	1338.87
1059.34	1407.33
1164.8	1452.13
1230.33	3061.03
1285.25	3166.69
1326.09	
1337.47	
1415.52	
1456.79	
3058.16	
3149.6	

Table S3: Vibrational frequencies of the reactants, pre-reactive complexes, transition states, product complexes, and products for the reaction calculated at the **MP2/cc-pVTZ level of theory.** All the frequency values are in cm^{-1}.

Reactant	OH	CR1A	TS1A	PC1A	P1A	H2O	CR2A	TS2A
24.93	3819.13	16.94	-2144.37	35.97	35.97	1652.08	18.53	-2211.71
120.2		46.88	22.94	48.55	48.55	3855.52	39.55	32.06
141.77		56.52	74.05	141.74	141.74	3975.84	57.29	71.06
230.54		93.13	91.28	217.54	217.54		95.54	86.06
240.29		101.6	132.27	227.12	227.12		110.6	133.19
304.58		135.81	151.67	311.68	311.68		138.14	143.2
329.4		149.43	163.4	330.85	330.85		145.46	163.28
385.13		231.8	230.77	335.62	335.62		231.07	229.66
409.07		241.45	233.43	389.79	389.79		241.03	243.94
468.78		296.22	306.13	462.6	462.6		291.24	304.98
539.03		306.78	326.48	494.87	494.87		305.56	325.39
550.24		330.58	341.55	545.14	545.14		330.1	354.95
655.79		386.53	395.15	610.36	610.36		386.91	391.98
706.63		413.68	469.42	659.15	659.15		416.18	470.82
839.21		470.22	540.51	778.43	778.43		468.89	532.56
890.83		538.96	546.29	831.67	831.67		539.39	549.84
930.93		550.72	656.72	881.57	881.57		550.42	656.56
1029.06		655.68	693.8	1017.01	1017.01		655.97	675.06
1177.02		708.41	778.02	1189.4	1189.4		702.28	760.91
1193.54		840.12	835.16	1208.65	1208.65		839.45	808.68
1223.37		887.16	870.92	1235.51	1235.51		889.25	846.81
1306.74		934.41	889.07	1291.57	1291.57		933.93	909.13
1339.23		1019.23	976.46	1435.4	1435.4		1030.92	977.35
1410.88		1175.67	1030.13	3312.24	3312.24		1174.3	1051.14
1460.4		1200.89	1110.35				1198.97	1131.82
3132.85		1214.34	1198.2				1222.23	1170.21
3202.72		1299.48	1213.89				1303.8	1207.22
		1341.33	1252.86				1341	1258.63
		1417.75	1302.01				1418.45	1295.01
		1461.63	1397.28				1465.23	1393.79
		3135.08	1468.52				3130.79	1459.89
		3204.77	3197.04				3201.43	3177.08
		3801.99	3785.42				3799.05	3788.5

PC2A	P2A	CR3A	TS3A	PC3A	P3A	HOCl	CR4A	TS4A
23.14	25.56	14.23	-592.25	19.94	30.96	769.36	13.61	-531.03
39	58.73	15.98	23.19	26.84	102.46	1278.29	33.05	25.88
49.57	142.32	25.53	64.91	33.51	140.07	3801.89	46.8	64.29
61.1	224.34	64.42	92.94	39.97	264.11		85.65	85.11
86.22	239.61	65.05	116.76	56.43	305.8		118.61	123.3
112.61	298.11	120.82	140.07	75.28	394.95		143	150.11
150.04	319.85	135.78	185.99	78.94	419.91		209.41	169.24
214.71	330.84	153.51	217.33	103.02	502.66		230.3	219.39
227.95	391.88	234.06	240.89	141.78	543.33		233.17	239.29
243.86	466.5	240.66	298.91	265.21	548.7		255	293.53
249.93	517.31	304.71	306.38	306.9	679.22		305.03	310.36
301.23	542.97	330.57	348.77	396.73	740.44		330.05	341.94
326.36	637.74	385.44	405.5	422.84	853.09		386.2	382.19
379.31	666.34	409.07	448.41	509.07	928.64		408.21	444.87
408.06	746.9	469.9	541.87	543.7	1060.72		469.6	545.65
466.62	852.03	538.96	547.8	550.15	1182.07		539.53	546.33
535.25	886.99	550.24	633.01	683.17	1212.72		551.39	653.71
542.86	1024.8	656.39	704.98	741.35	1271.22		656.07	691.18
655.62	1174.82	705.63	754.16	799.41	1310.69		706.18	812.22
667.17	1201.39	841.67	862.24	854.22	1343.36		840.51	864.71
748.2	1226.48	891.31	928.26	928.53	1390.43		894.13	931.67
850.42	1319.75	931.7	1049.88	1061.21	1458		924.51	1036.43
885.33	1430.05	1027.71	1161.6	1183.53	3126.15		1027.16	1161.23
1024.94	3299.45	1176.3	1182.83	1213.79	3195.68		1170.34	1179.64
1156.74		1193.32	1202.67	1271.09			1202.92	1201.84
1189.63		1221.77	1255.15	1274.7			1214.58	1252.95
1229.33		1306.75	1302.6	1309.6			1304.23	1303.17
1324.98		1338.85	1336.82	1342.03			1332.8	1327.1
1434.35		1411.61	1397.3	1390.85			1411.99	1408.55
1654.65		1460.17	1455.7	1455.22			1460.92	1457.94
3284.21		3132.55	3131.76	3127.11			3132.93	3110.63
3838.08		3202.14	3201.27	3195.76			3202.97	3189.42
3953.38		3811.2	3814.94	3798.07			3812.9	3815.29

PC4A	P4A	HCl	CR1B	TS1B	PC1B	P1B	CR2B	TS2B
22.8	30.4	3054.58	18.4	-1326.04	15.02	36.04	19.62	-1271.28
33.99	89.9		27.27	19.73	25.77	48.58	26.79	24.99
35.38	143.35		36.28	49.81	45.03	141.74	46.16	51.31
41.28	262.64		51.8	77.24	55.78	217.54	51.74	70.12
62.05	310.43		121.96	118.23	76	227.14	126.41	111.88
108.62	364.45		141.41	150.77	138.55	311.68	142	141.32
118.52	435.31		231.25	215.03	152.74	330.86	230.85	226.15
143.63	439.46		241.01	228.11	210.24	335.59	240.31	240.77
262.23	545.26		304.69	299.11	219.86	389.78	304.91	300.64
292.76	552.42		328.94	314.47	232.3	462.6	329.42	311.97
311.77	659.15		384.53	329.05	311.89	494.82	386.07	350.24
368.32	817.3		409.16	392.5	332.05	545.14	411.16	390.21
438.76	865.09		467.41	469.09	335.37	610.31	468.43	463.52
439.06	921.57		539.08	502.76	389.08	659.14	538.64	490
547.91	1058.59		550.19	545.44	463.04	778.42	550.09	537.24
553.27	1165.48		654.91	551.79	492.42	831.65	655.87	553.08
658.81	1214.63		707.1	658.14	545.18	881.57	700.67	662.49
767.65	1266.85		834.6	732.76	607.4	1017	840.28	702.29
822.01	1316.83		889.64	845.17	658.74	1189.32	889.87	822.16
859.5	1332.32		930.02	851.59	775.92	1208.66	931.98	850.78
923.78	1408.32		1029.91	874.32	834.69	1235.51	1028.03	859.55
1059.72	1460		1178.48	926.71	879.01	1291.55	1175.54	917.81
1156.13	3090.29		1195.72	1008.12	1015.81	1435.4	1195.21	1058.85
1214.2	3194.24		1224.9	1097.4	1163.29	3312.31	1224.33	1103.72
1254.03			1307.13	1206.15	1215.35		1306.03	1165.61
1293.22			1340.55	1219.18	1232.25		1339.27	1204.52
1314.29			1411.62	1230.06	1291.08		1412.6	1241.61
1332.82			1461.13	1307.36	1437.84		1460.91	1300.82
1414.5			3132.24	1392.77	3034.28		3132.48	1392
1464.46			3202.35	3221.95	3316.96		3203.3	3207.56
3085.97								
3192.94								
3776.23								

PC2B	P2B	CR3B	TS3B	PC3B	P3B	Cl_2
17.73	25.54	18.39	-438.26	20.65	30.94	577.97
26.31	58.75	27.24	25.62	24.12	102.46	
40.91	142.33	36.27	49.69	37.06	140.07	
68.98	224.34	51.82	64.18	50.02	264.11	
77.44	239.6	121.99	109.19	69.23	305.8	
145.14	298.11	141.43	124.47	73.66	394.95	
167.92	319.87	231.25	153.79	103.36	419.91	
224.98	330.86	241	189.46	142.33	502.68	
239.37	391.88	304.69	257.07	265.41	543.33	
271.17	466.5	328.94	276.67	307.09	548.7	
299.4	517.33	384.52	316.84	396.86	679.24	
324.94	542.98	409.17	403.62	423.4	740.44	
338.73	637.78	467.41	445.79	510.68	853.1	
391.59	666.34	539.08	538.15	543.8	928.65	
465.56	746.91	550.19	546.62	550.45	1060.73	
518.62	852.02	654.9	572.5	565.13	1182.08	
542.49	886.98	707.11	696.88	684.59	1212.71	
638.3	1024.79	834.6	744.77	741.81	1271.23	
667.92	1174.82	889.63	861.57	854.65	1310.7	
737.55	1201.4	930.04	932.73	929.2	1343.36	
853.38	1226.5	1029.9	1062.4	1062.74	1390.42	
884.34	1319.75	1178.48	1190.14	1184.18	1458	
1027.15	1430.05	1195.72	1211.35	1214.52	3126.15	
1175.44	3299.43	1224.9	1273.88	1272.53	3195.68	
1206.63		1307.12	1302.99	1309.24		
1230.36		1340.56	1339.72	1342.8		
1317.27		1411.62	1387.03	1389.56		
1430.92		1461.13	1455.66	1455.31		
2995.54		3132.24	3136.47	3125.91		
3300.5		3202.35	3207.27	3195.15		

CR4B	TS4B	PC4B	P4B
10.66	-438.95	11.19	31.17
16.41	30.37	20.31	80.62
31.53	44.43	33.43	140.9
47.05	69.88	38.21	262.38
119.66	105.46	42.35	311.33
142.14	142.73	48.32	362.71
230.87	158.56	92.08	416.81
240.8	188.93	144.24	438.07
304.67	267.3	262.56	543.45
329.43	272.2	310.42	551.24
385.54	318.45	365.07	656.45
408.58	369.71	438.78	804
468.96	446.84	441.52	873.79
539.23	511.21	545.6	924.26
550.42	545.75	552.97	1064.4
655.29	563.9	570.12	1167.09
705.18	663.81	659.79	1233.11
839.67	820.15	821.86	1282.71
891.33	866.71	865.74	1327.63
928.19	930.02	922.28	1338.87
1027.37	1049.06	1058.49	1407.33
1173.76	1164.57	1165.34	1452.13
1197.22	1206.07	1214.98	3061.03
1218.02	1278.52	1266.76	3166.69
1304.19	1306.76	1315.67	
1333.46	1330.95	1331.42	
1410.77	1409.22	1408.51	
1460.44	1455.45	1459.25	
3132.8	3102.33	3088.3	
3202.86	3187.24	3192.91	

Table S4: The corrected zero-point energies (EE+ZPE), enthalpies (H), and Gibbs free energies (G) of all the species calculated at the **M06-2X/cc-pVTZ level of theory.** All energies are in Hartree.

Reaction Pathway	Species	EE+ZPE	H	G
Reactants	$CF_3CH_2CFCl_2$	-1435.2925	-1435.2829	-1435.3279
	OH	-75.7219	-75.7186	-75.7388
R1A	CR1A	-1511.0210	-1511.0083	-1511.0614
	TS1A	-1511.0100	-1510.9980	-1511.0498
	PC1A	-1511.0457	-1511.0320	-1511.0876
	P1A	-1434.6345	-1434.6245	-1434.6718
	H_2O	-76.4037	-76.3999	-76.4220
R2A	CR2A	-1511.0213	-1511.0087	-1511.0612
	TS2A	-1511.0093	-1510.9973	-1511.0485
	PC2A	-1511.0447	-1511.0309	-1511.0870
	P2A	-1434.6329	-1434.6230	-1434.6699
R3A	CR3A	-1511.0211	-1511.0083	-1511.0615
	TS3A	-1510.9779	-1510.9655	-1511.0190
	PC3A	-1510.9853	-1510.9718	-1511.0298
	P3A	-975.0301	-975.0215	-975.0650
	HOCl	-535.9508	-535.9470	-535.9737
R4A	CR4A	-1511.0210	-1511.0084	-1511.0612
	TS4A	-1510.9757	-1510.9634	-1511.0160
	PC4A	-1510.9840	-1510.9713	-1511.0271
	P4A	-975.0299	-975.0212	-975.0650
R1B	Cl	-460.1407	-460.1383	-460.1564
	CR1B	-1895.4391	-1895.4271	-1895.4807
	TS1B	-1895.4239	-1895.4122	-1895.4642
	PC1B	-1895.4366	-1895.4232	-1895.4800
	P1B	-1434.6330	-1434.6230	-1434.6700
	HCl	-460.7997	-460.7964	-460.8175
R2B	CR2B	-1895.4393	-1895.4274	-1895.4798
	TS2B	-1895.4214	-1895.4097	-1895.4615
	PC2B	-1895.4364	-1895.4231	-1895.4786
	P2B	-1434.6329	-1434.6230	-1434.6699
R3B	CR3B	-1895.4390	-1895.4270	-1895.4270
	TS3B	-1895.4053	-1895.3923	-1895.4469
	PC3B	-1895.4074	-1895.3945	-1895.4518
	P3B	-975.0301	-975.0215	-975.0650
	Cl_2	-920.3730	-920.3695	-920.3947
R4B	CR4B	-1895.4393	-1895.4274	-1895.4797
	TS4B	-1895.4022	-1895.3902	-1895.4432
	PC4B	-1895.4059	-1895.3930	-1895.4504
	P4B	-975.0299	-975.0212	-975.0649

Table S5: The corrected zero-point energies (EE+ZPE), enthalpies (H), and Gibbs free energies (G) of all the species calculated at the **MP2/cc-pVTZ level of theory.** All energies are in Hartree.

Reaction Pathway	Species	EE+ZPE	H	G
Reactants	**$CF_3CH_2CFCl_2$**	-1433.5659	-1433.5563	-1433.6016
	OH	-75.6102	-75.6069	-75.6271
R1A	**CR1A**	-1509.1814	-1509.1683	-1509.2234
	TS1A	-1509.1663	-1509.1544	-1509.2058
	PC1A	-1509.2078	-1509.1939	-1509.2503
	P1A	-1432.9047	-1432.8948	-1432.9416
	H_2O	-76.2970	-76.2932	-76.3153
R2A	**CR2A**	-1509.1812	-1509.1680	-1509.2231
	TS2A	-1509.1656	-1509.1537	-1509.2049
	PC2A	-1509.2073	-1509.1934	-1509.2505
	P2A	-1432.9033	-1432.8933	-1432.9402
R3A	**CR3A**	-1509.1779	-1509.1642	-1509.223
	TS3A	-1509.1251	-1509.1132	-1509.1649
	PC3A	-1509.1411	-1509.1274	-1509.1868
	P3A	-973.7935	-973.7849	-973.8282
	HOCl	-535.3442	-535.3404	-535.3672
R4A	**CR4A**	-1509.1787	-1509.1656	-1509.2213
	TS4A	-1509.1235	-1509.1115	-1509.1632
	PC4A	-1509.1440	-1509.1307	-1509.1880
	P4A	-973.7936	-973.7849	-973.8285
R1B	**Cl**	-459.6433	-459.6410	-459.6590
	CR1B	-1893.2119	-1893.1997	-1893.2546
	TS1B	-1893.1960	-1893.1843	-1893.2361
	PC1B	-1893.2102	-1893.1966	-1893.2545
	P1B	-1432.9047	-1432.8948	-1432.9416
	HCl	-460.3024	-460.2991	-460.3203
R2B	**CR2B**	-1893.2120	-1893.1999	-1893.2544
	TS2B	-1893.1938	-1893.1822	-1893.2338
	PC2B	-1893.2090	-1893.1955	-1893.2526
	P2B	-1432.9033	-1432.8933	-1432.9402
R3B	**CR3B**	-1893.2119	-1893.1997	-1893.2546
	TS3B	-1893.1663	-1893.1545	-1893.2072
	PC3B	-1893.1723	-1893.1594	-1893.2170
	P3B	-973.7935	-973.7849	-973.8282
	Cl_2	-919.3754	-919.3719	-919.3972
R4B	**CR4B**	-1893.2110	-1893.1987	-1893.2549
	TS4B	-1893.1633	-1893.1515	-1893.2039
	PC4B	-1893.1715	-1893.1584	-1893.2182
	P4B	-973.7935	-973.7849	-973.8285

Table S6: Intrinsic reaction coordinate (IRC) data for the reaction of DTP with OH-radical calculated at the **MP2/cc-pVTZ level of theory (R1A).**

Coordinates	Energy (Hartree)	Relative Energy (Hartree)	Relative Energy (kcal/mol)
-2.07362	-1509.2589	-0.0193	-12.1672
-1.96971	-1509.2584	-0.0188	-11.8409
-1.86589	-1509.2578	-0.0183	-11.5020
-1.76207	-1509.2573	-0.0177	-11.1506
-1.65842	-1509.2567	-0.0171	-10.7867
-1.5548	-1509.2561	-0.0165	-10.4102
-1.45126	-1509.2555	-0.0159	-10.0023
-1.34757	-1509.2548	-0.0152	-9.5693
-1.24378	-1509.2540	-0.0145	-9.1050
-1.13991	-1509.2532	-0.0136	-8.5904
-1.03600	-1509.2523	-0.0127	-8.0257
-0.93207	-1509.2513	-0.0117	-7.3919
-0.82815	-1509.2501	-0.0106	-6.6703
-0.72423	-1509.2488	-0.0093	-5.8483
-0.62038	-1509.2473	-0.0078	-4.9070
-0.51885	-1509.2455	-0.0059	-3.7273
-0.41593	-1509.2423	-0.0027	-1.7193
-0.31202	-1509.2375	0.0020	1.2801
-0.20802	-1509.2321	0.0073	4.6309
-0.10401	-1509.2283	0.0112	7.0656
0	-1509.2271	0.0124	7.7998
0.10366	-1509.2278	0.0117	7.3794
0.20534	-1509.2289	0.0106	6.6828
0.30907	-1509.2298	0.0097	6.0867
0.41298	-1509.2307	0.0088	5.5220
0.51698	-1509.2316	0.0079	4.9823
0.62085	-1509.2324	0.0071	4.4615
0.72431	-1509.2332	0.0063	3.9720
0.82694	-1509.2339	0.0056	3.5140
0.92956	-1509.2346	0.0049	3.1061
1.03327	-1509.2352	0.0043	2.7108
1.13721	-1509.2358	0.00373	2.3405
1.24118	-1509.2363	0.00319	2.0017
1.34517	-1509.2368	0.00268	1.6817
1.44916	-1509.2373	0.00222	1.3930
1.55314	-1509.2377	0.00178	1.1169
1.65712	-1509.2381	0.00138	0.8659
1.76111	-1509.2385	0.00100	0.6275
1.86509	-1509.2389	0.00065	0.4078
1.96908	-1509.2392	0.00031	0.1945
2.07306	-1509.2395	0	0.0000

Table S7: Intrinsic reaction coordinate (IRC) data for the reaction of DTP with OH-radical calculated at the **MP2/cc-pVTZ level of theory (R2A)**.

Coordinates	Energy (Hartree)	Relative Energy (Hartree)	Relative Energy (kcal/mol)
-2.07002	-1509.2555	-0.0163	-10.2408
-1.96626	-1509.2550	-0.0158	-9.9270
-1.86251	-1509.2545	-0.0153	-9.6070
-1.75876	-1509.2540	-0.0147	-9.2681
-1.65509	-1509.2534	-0.0142	-8.9167
-1.55155	-1509.2528	-0.0136	-8.5528
-1.44824	-1509.2522	-0.0130	-8.1700
-1.34496	-1509.2516	-0.0123	-7.7684
-1.24150	-1509.2509	-0.0116	-7.3292
-1.13789	-1509.2501	-0.0109	-6.8585
-1.03420	-1509.2493	-0.0101	-6.3377
-0.93050	-1509.2484	-0.0091	-5.7667
-0.82679	-1509.2473	-0.0081	-5.1141
-0.72308	-1509.2462	-0.0069	-4.3736
-0.61940	-1509.2448	-0.0055	-3.5077
-0.51694	-1509.2431	-0.0039	-2.4723
-0.41503	-1509.2405	-0.0012	-0.8094
-0.31141	-1509.2363	0.0029	1.8385
-0.20762	-1509.2313	0.0079	4.9760
-0.10382	-1509.2274	0.0117	7.3856
0	-1509.2262	0.0129	8.1449
0.10356	-1509.2269	0.0122	7.6868
0.20524	-1509.2281	0.0110	6.9338
0.30845	-1509.2291	0.0100	6.3126
0.41222	-1509.2300	0.0091	5.7416
0.51594	-1509.2309	0.0082	5.1894
0.61960	-1509.2317	0.0074	4.6686
0.72275	-1509.2325	0.0066	4.1666
0.82536	-1509.2333	0.0059	3.7022
0.92832	-1509.2340	0.0052	3.2692
1.03183	-1509.2346	0.0045	2.8614
1.13553	-1509.2352	0.0039	2.4786
1.23931	-1509.2358	0.0033	2.1209
1.34310	-1509.2363	0.0028	1.7883
1.44691	-1509.2368	0.0023	1.4746
1.55071	-1509.2373	0.0018	1.1859
1.65451	-1509.2377	0.0014	0.9161
1.75831	-1509.2381	0.0010	0.6651
1.86211	-1509.2385	0.0006	0.4329
1.96591	-1509.2389	0.0003	0.2070
2.06972	-1509.2392	0.0000	0.0000

Table S8: Intrinsic reaction coordinate (IRC) data for the abstraction of Cl-atom of DTP by OH-radical calculated at the **MP2/cc-pVTZ level of theory (R3A)**.

Coordinates	Energy (Hartree)	Relative energy (Hartree)	Relative energy (kcal/mol)
-7.07136	-1509.2067	0.000	0.0000
-6.88454	-1509.2066	0.0002	0.1568
-6.47844	-1509.2063	0.0005	0.3514
-6.06984	-1509.2060	0.0009	0.6149
-5.66289	-1509.2056	0.0015	0.9412
-5.25534	-1509.2051	0.0021	1.3491
-4.84726	-1509.2045	0.0029	1.8574
-4.43896	-1509.2039	0.0039	2.4660
-4.02844	-1509.2031	0.0064	4.0724
-3.61786	-1509.2023	0.0082	5.1831
-3.22076	-1509.2017	0.0104	6.5385
-2.83481	-1509.2007	0.0130	8.2139
-2.44527	-1509.1996	0.0164	10.3161
-2.04159	-1509.1983	0.0205	12.9139
-1.63318	-1509.1970	0.0255	16.0389
-1.22209	-1509.1957	0.0312	19.6156
-0.81514	-1509.1941	0.0374	23.4998
-0.40347	-1509.1928	0.0435	27.3025
0	-1509.1919	0.0479	30.0886
0.41343	-1509.1934	0.0493	30.9796
0.82751	-1509.1978	0.0485	30.4651
1.24176	-1509.2039	0.0471	29.5929
1.65643	-1509.2100	0.0456	28.6391
2.07121	-1509.2157	0.0442	27.7794
2.48595	-1509.2207	0.0429	26.9574
2.90051	-1509.2249	0.0416	26.1479
3.31463	-1509.2282	0.0406	25.4953
3.72856	-1509.2309	0.0395	24.8301
4.1417	-1509.2330	0.0389	24.4662
4.55342	-1509.2348	0.0381	23.9579
4.96091	-1509.2362	0.0374	23.4998
5.37373	-1509.2374	0.0367	23.0731
5.78729	-1509.2383	0.0362	22.7343
6.20159	-1509.2392	0.0357	22.4268
6.6156	-1509.2398	0.0353	22.1695
7.02797	-1509.2403	0.0349	21.9499
7.43734	-1509.2407	0.0346	21.7617
7.84261	-1509.2411	0.0345	21.6989

Table S9: Intrinsic reaction coordinate (IRC) data for the abstraction of Cl-atom of DTP by OH-radical calculated at the **MP2/cc-pVTZ level of theory (R4A).**

Coordinates	Energy (Hartree)	Relative Energy (Hartree)	Relative Energy (kcal/mol)
-7.42180	-1509.2405	0.0000	0.0000
-7.05059	-1509.2401	0.0004	0.2572
-6.67983	-1509.2396	0.0009	0.5710
-6.30866	-1509.2390	0.0015	0.9600
-5.93808	-1509.2383	0.0022	1.4181
-5.57201	-1509.2374	0.0030	1.9327
-5.20737	-1509.2364	0.0040	2.5602
-4.83736	-1509.2352	0.0053	3.3383
-4.46917	-1509.2337	0.0067	4.2544
-4.09920	-1509.2320	0.0085	5.3588
-3.72871	-1509.2299	0.0106	6.6954
-3.35631	-1509.2273	0.0132	8.3081
-2.98371	-1509.2241	0.0163	10.2784
-2.61057	-1509.2203	0.0201	12.6629
-2.23728	-1509.2158	0.0246	15.4867
-1.86393	-1509.2107	0.0297	18.6932
-1.49062	-1509.2052	0.0353	22.1821
-1.11748	-1509.1995	0.0410	25.7400
-0.74461	-1509.1944	0.0460	28.9152
-0.37202	-1509.1912	0.0493	30.9545
0	-1509.1903	0.0502	31.5444
0.36603	-1509.1908	0.0497	31.1930
0.73678	-1509.1919	0.0486	30.5153
1.10004	-1509.1932	0.0473	29.6870
1.45671	-1509.1943	0.0462	29.0156
1.82351	-1509.1954	0.0451	28.3002
2.19055	-1509.1964	0.0441	27.6790
2.56350	-1509.1974	0.0430	27.0327
2.93471	-1509.1984	0.0421	26.4491
3.30649	-1509.1992	0.0413	25.9283
3.67895	-1509.2000	0.0405	25.4451
4.05176	-1509.2007	0.0398	25.0058
4.4248	-1509.2013	0.0392	24.6105
4.79787	-1509.2019	0.0386	24.2466
5.16998	-1509.2024	0.0381	23.9140
5.53898	-1509.2029	0.0376	23.6191
5.90356	-1509.2033	0.0372	23.3618
6.25711	-1509.2036	0.0369	23.1798
6.62842	-1509.2039	0.0366	22.9790
7.00071	-1509.2042	0.0363	22.7845
7.37260	-1509.2045	0.03603	22.6088

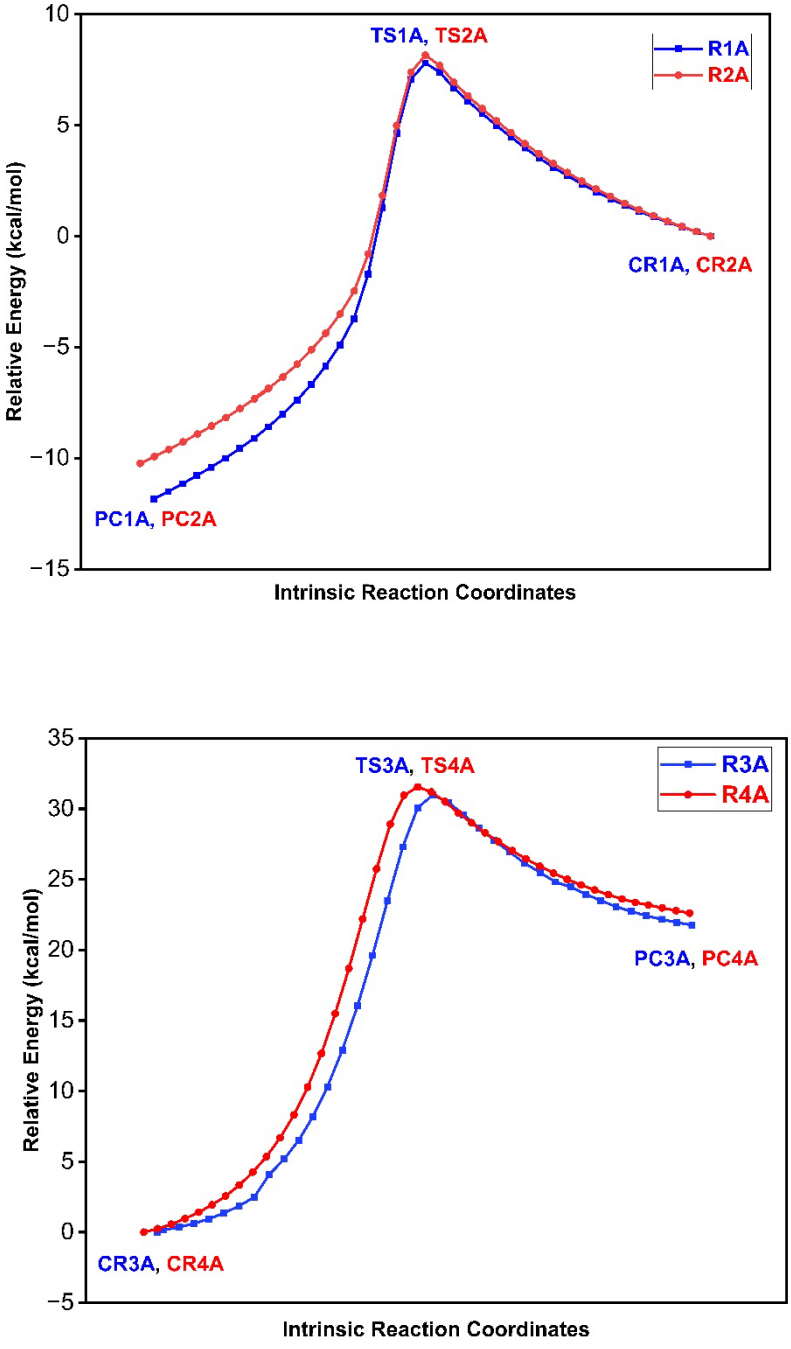

Figure S3: Intrinsic reaction coordinate (IRC) plots for R1A-R2A and R3A-R4A at the **MP2/cc-pVTZ level of theory**.

Table S10: Intrinsic reaction coordinate (IRC) data for the abstraction of H-atom of DTP by Cl-atom calculated at the **MP2/cc-pVTZ level of theory (R1B).**

Coordinates	Energy (Hartree)	Relative Energy (Hartree)	Relative Energy (kcal/mol)
-2.17647	-1893.2498	-0.0063	0.0069
-2.06740	-1893.2495	-0.0061	0.0072
-1.95834	-1893.2493	-0.0058	0.0074
-1.84929	-1893.2491	-0.0056	0.0076
-1.74029	-1893.2488	-0.0053	0.0079
-1.63139	-1893.2485	-0.0051	0.0082
-1.52249	-1893.2483	-0.0048	0.0084
-1.41359	-1893.2480	-0.0045	0.0087
-1.30460	-1893.2477	-0.0042	0.0090
-1.19557	-1893.2474	-0.0039	0.0093
-1.08651	-1893.2471	-0.0036	0.0096
-0.97745	-1893.2468	-0.0033	0.0099
-0.86838	-1893.2465	-0.0030	0.0102
-0.75933	-1893.2461	-0.0027	0.0106
-0.65030	-1893.2458	-0.0023	0.0109
-0.54131	-1893.2454	-0.0020	0.0113
-0.43237	-1893.2451	-0.0016	0.0116
-0.32360	-1893.2446	-0.0012	0.0121
-0.21484	-1893.2440	-0.0007	0.0125
-0.10819	-1893.2438	-0.0002	0.0130
0	-1893.2434	0.0000	0.0133
0.10899	-1893.2435	-0.0004	0.0128
0.21803	-1893.2454	-0.0020	0.0113
0.32706	-1893.2476	-0.0041	0.0091
0.43579	-1893.2496	-0.0061	0.0071
0.53719	-1893.2505	-0.0071	0.0062
0.64521	-1893.2511	-0.0076	0.0056
0.75363	-1893.2516	-0.0082	0.0051
0.86242	-1893.2521	-0.0087	0.0046
0.97132	-1893.2526	-0.0091	0.0041
1.08019	-1893.2531	-0.0096	0.0036
1.18905	-1893.2535	-0.0101	0.0032
1.29787	-1893.2540	-0.0105	0.0027
1.40670	-1893.2544	-0.0109	0.0023
1.51554	-1893.2548	-0.0113	0.0019
1.62444	-1893.2551	-0.0117	0.0016
1.73336	-1893.2555	-0.0120	0.0012
1.84233	-1893.2558	-0.0123	0.0009
1.95132	-1893.2561	-0.0127	0.0006
2.06034	-1893.2564	-0.0130	0.0003
2.16936	-1893.2567	-0.0133	0.0000

Table S11: Intrinsic reaction coordinate (IRC) data for the abstraction of H-atom of DTP by Cl-atom calculated at the **MP2/cc-pVTZ level of theory (R2B).**

Coordinates	Energy (Hartree)	Relative Energy (Hartree)	Relative Energy (kcal/mol)
-2.30775	-1893.2474	-0.0063	0.0090
-2.19761	-1893.2472	-0.0060	0.0092
-2.08746	-1893.2469	-0.0058	0.0095
-1.97731	-1893.2467	-0.0055	0.0097
-1.86717	-1893.2464	-0.0053	0.0100
-1.75703	-1893.2462	-0.0050	0.0102
-1.64691	-1893.2459	-0.0048	0.0105
-1.53680	-1893.2456	-0.0045	0.0108
-1.42673	-1893.2453	-0.0042	0.0110
-1.31666	-1893.2450	-0.0039	0.0113
-1.20662	-1893.2447	-0.0036	0.0116
-1.09654	-1893.2444	-0.0033	0.0119
-0.98646	-1893.2441	-0.0030	0.0123
-0.87634	-1893.2438	-0.0027	0.0126
-0.76623	-1893.2435	-0.0024	0.0129
-0.65610	-1893.2432	-0.0020	0.0132
-0.54602	-1893.2428	-0.0017	0.0136
-0.43595	-1893.2425	-0.0013	0.0139
-0.32614	-1893.2421	-0.0010	0.0143
-0.21622	-1893.2420	-0.0006	0.0014
-0.10841	-1893.2418	-0.0002	0.0015
0	-1893.2411	0.0000	0.0153
0.11001	-1893.2420	-0.0004	0.0014
0.22012	-1893.2432	-0.0021	0.0132
0.33025	-1893.2458	-0.0047	0.0106
0.44029	-1893.2484	-0.0072	0.0080
0.54710	-1893.2499	-0.0088	0.0064
0.65461	-1893.2506	-0.0095	0.0058
0.76429	-1893.2512	-0.0101	0.0052
0.87416	-1893.2517	-0.0106	0.0046
0.98403	-1893.2523	-0.0111	0.0041
1.09367	-1893.2528	-0.0116	0.0036
1.20322	-1893.2532	-0.0121	0.0031
1.31274	-1893.2537	-0.0126	0.0027
1.42249	-1893.2541	-0.0130	0.0022
1.53238	-1893.2546	-0.0135	0.0018
1.64234	-1893.2550	-0.0139	0.0014
1.75236	-1893.2554	-0.0142	0.0010
1.86240	-1893.2557	-0.0146	0.0006
1.97245	-1893.2561	-0.0150	0.0003
2.08251	-1893.2564	-0.0153	0.0000

Table S12: Intrinsic reaction coordinate (IRC) data for the abstraction of Cl-atom of DTP with Cl-atom calculated at the **MP2/cc-pVTZ level of theory (R3B).**

Coordinates	Energy (Hartree)	Relative Energy (Hartree)	Relative Energy (kcal/mol)
10.1109	-1893.2673	-0.0003	-0.1882
9.6361	-1893.2670	-0.0005	-0.0251
9.1559	-1893.2667	0.0002	0.1694
8.6738	-1893.2664	0.0006	0.3890
8.1915	-1893.2660	0.0010	0.6526
7.7090	-1893.2655	0.0015	0.9663
7.2266	-1893.2649	0.0021	1.3303
6.7441	-1893.2642	0.0028	1.7632
6.2617	-1893.2634	0.0036	2.2652
5.7793	-1893.2625	0.0045	2.8488
5.2969	-1893.2614	0.0056	3.5265
4.8149	-1893.2601	0.0068	4.3109
4.3338	-1893.2586	0.0083	5.2396
3.8538	-1893.2568	0.0102	6.4005
3.3735	-1893.2543	0.0126	7.9378
2.8922	-1893.2510	0.0160	10.0462
2.4108	-1893.2465	0.0204	12.8512
1.9286	-1893.2407	0.0261	16.4154
1.4465	-1893.2307	0.0326	20.4816
0.9642	-1893.2285	0.0385	24.1650
0.4819	-1893.2248	0.0422	26.4993
0	-1893.2237	0.0433	27.1833
-0.4721	-1893.2242	0.0427	26.8381
-0.9437	-1893.2251	0.0419	26.3173
-1.4222	-1893.2258	0.0412	25.8718
-1.8915	-1893.2265	0.0405	25.4388
-2.3643	-1893.2270	0.0399	25.0874
-2.8427	-1893.2275	0.0394	24.7737
-3.3241	-1893.2280	0.0390	24.4913
-3.8062	-1893.2283	0.0386	24.2528
-4.2886	-1893.2287	0.0383	24.0521
-4.7711	-1893.2289	0.0380	23.8889
-5.2536	-1893.2291	0.0378	23.7571
-5.7360	-1893.2293	0.0377	23.6567
-6.2185	-1893.2294	0.0375	23.5814
-6.7010	-1893.2295	0.0375	23.5312

Table S13: Intrinsic reaction coordinate (IRC) data for the abstraction of Cl-atom of DTP with Cl-atom calculated at the **MP2/cc-pVTZ level of theory (R4B).**

Coordinates	Energy (Hartree)	Relative Energy (Hartree)	Relative Energy (kcal/mol)
-6.52843	-1893.2243	0.0396	24.8866
-6.11564	-1893.2242	0.0398	24.9933
-5.70286	-1893.2240	0.0400	25.1188
-5.2901	-1893.2237	0.0402	25.2631
-4.87747	-1893.2235	0.0405	25.4263
-4.465	-1893.2232	0.0408	25.6145
-4.05314	-1893.2228	0.0411	25.8279
-3.64258	-1893.2225	0.0415	26.0538
-3.23658	-1893.2221	0.0419	26.3048
-2.82771	-1893.2216	0.0423	26.5997
-2.42203	-1893.2211	0.0428	26.9009
-2.01535	-1893.2206	0.04340	27.2335
-1.62683	-1893.2201	0.0439	27.5660
-1.22628	-1893.2194	0.0446	28.0053
-0.81507	-1893.2187	0.0453	28.4508
-0.40757	-1893.2179	0.0460	28.9152
0	-1893.2175	0.0465	29.1850
0.4124	-1893.2183	0.0457	28.6893
0.82506	-1893.2211	0.0429	26.9197
1.23782	-1893.2259	0.0380	23.8889
1.65055	-1893.2319	0.0321	20.1615
2.06312	-1893.2377	0.0262	16.4969
2.47556	-1893.2427	0.0213	13.3845
2.88785	-1893.2466	0.0173	10.8871
3.29987	-1893.2497	0.0142	8.9544
3.71134	-1893.2521	0.0119	7.4923
4.1223	-1893.2539	0.0101	6.3565
4.53375	-1893.2553	0.0086	5.4341
4.94599	-1893.2566	0.0074	4.6497
5.35865	-1893.2577	0.0063	3.9532
5.77146	-1893.2587	0.0053	3.3445
6.18431	-1893.2595	0.0044	2.8112
6.59717	-1893.2603	0.0037	2.3405
7.01003	-1893.2609	0.0030	1.9264
7.42289	-1893.2615	0.0024	1.5562
7.83574	-1893.2620	0.0019	1.2424
8.24859	-1893.2625	0.0015	0.9600
8.66142	-1893.2629	0.0011	0.7153
9.07414	-1893.2632	0.0008	0.5020
9.48633	-1893.2635	0.00049	0.3074
9.89681	-1893.2638	0.00023	0.1443
10.30507	-1893.2640	0	0

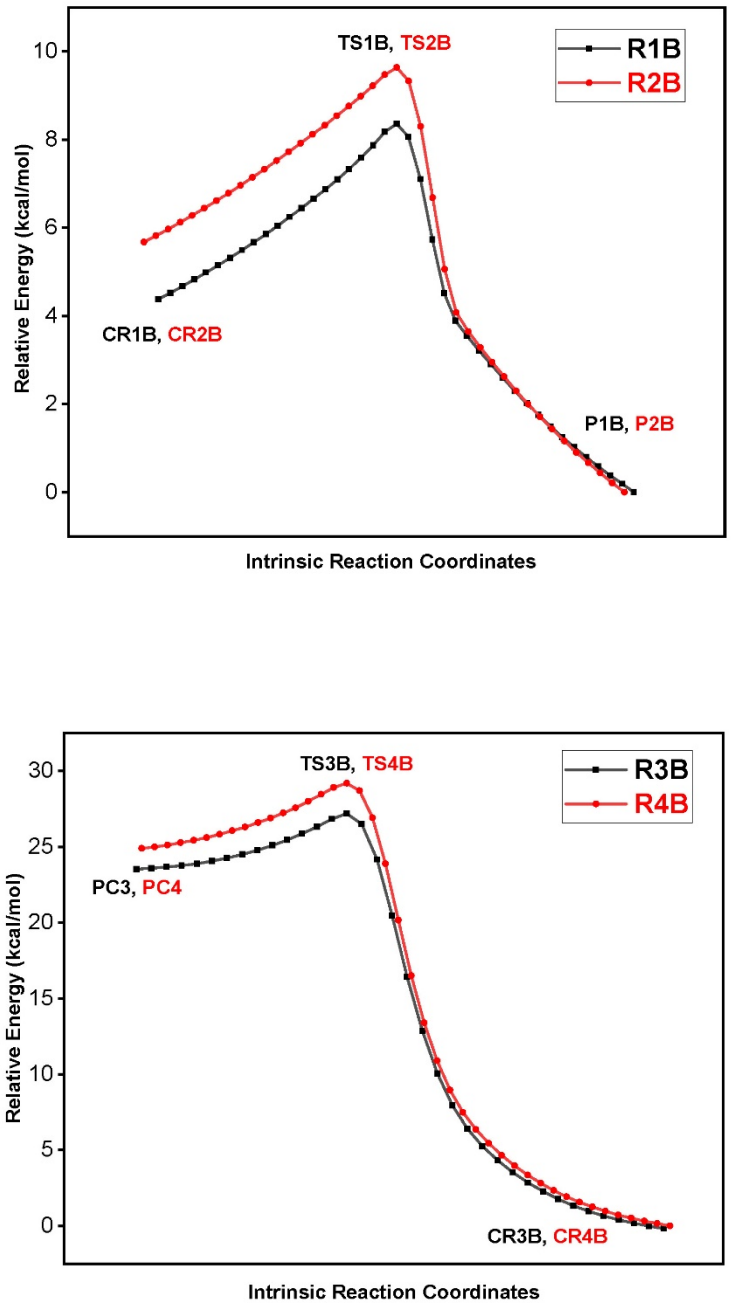

Figure S4: Intrinsic reaction coordinate (IRC) plots for the R1B-R2B and R3B-R4B at the **MP2/cc-pVTZ level of theory**.

Table S14: Single point energy calculated at the **CCSD(T)/aug-cc-pVTZ//MP2/cc-pVTZ level of theory** of all the species involved in the reaction (A).

Reactions	Species	Energy (kcal/mol)
$CF_3CH_2CCl_2F + {}^{\bullet}OH$	**Reactants**	-1509.4323
Reaction 1A	**CR1A**	-1509.4384
	TS1A	-1509.4221
	PC1A	-1509.4602
	P1A+H_2O	-1509.4533
Reaction 2A	**CR2A**	-1509.4383
	TS2A	-1509.4214
	PC2A	-1509.4594
	P2A+H_2O	-1509.4520
Reaction 3A	**CR3A**	-1509.4345
	TS3A	-1509.3924
	PC3A	-1509.4002
	P3A+HOCl	-1509.3952
Reaction 4A	**CR4A**	-1509.4364
	TS4A	-1509.3905
	PC4A	-1509.4029
	P4A+HOCl	-1509.3948

Table S15: Single point energy calculated at the **CCSD(T)/aug-cc-pVTZ//MP2/cc-pVTZ level of theory** of all the species involved in the reaction (B).

Reaction	Species	Energy (kcal/mol)
$CF_3CH_2CCl_2F$ + Cl	**Reactants**	-1893.4630
Reaction 1B	**CR1B**	-1893.4671
	TS1B	-1893.4438
	PC1B	-1893.4588
	P1B+HCl	-1893.4543
Reaction 2B	**CR2B**	-1893.4674
	TS2B	-1893.4417
	PC2B	-1893.4580
	P2B+HCl	-1893.4530
Reaction 3B	**CR3B**	-1893.4671
	TS3B	-1893.4274
	PC3B	-1893.4290
	P3B+Cl_2	-1893.4239
Reaction 4B	**CR4B**	-1893.4655
	TS4B	-1893.4245
	PC4B	-1893.4275
	P4B+Cl_2	-1893.4237

Table S16: Relative energies of the species involved in the reaction of DTP with ˙OH and Cl at the **CCSD(T)/aug-cc-pVTZ//MP2/cc-pVTZ** level of theory. Energies are in kcal/mol.

Species	Relative Energy	Species	Relative Energy
$CCl_2FCH_2CF_3$ (DTP) + ˙OH		**$CCl_2FCH_2CF_3$ (DTP) + Cl**	
R (DTP + ˙OH)	0.00	**R (DTP + Cl)**	0.00
CR1A	-3.79	**CR1B**	-2.58
TS1A	6.36	**TS1B**	12.07
PC1A	-17.49	**PC1B**	2.63
P1A + H_2O	-13.17	**P1B + H_2O**	5.48
CR2A	-3.75	**CR2B**	-2.75
TS2A	6.80	**TS2B**	13.38
PC2A	-16.97	**PC2B**	3.15
P2A + H_2O	-12.36	**P2B + H_2O**	6.29
CR3A	-1.36	**CR3B**	-2.59
TS3A	25.08	**TS3B**	22.30
PC3A	20.17	**PC3B**	21.34
P3A + HOCl	23.27	**P3B + HOCl**	24.51
CR4A	-2.55	**CR4B**	-1.55
TS4A	26.27	**TS4B**	24.13
PC4A	18.48	**PC4B**	22.25
P4A + HOCl	23.56	**P4B + HOCl**	24.63

Figure 4 of the manuscript has been prepared using this data.

Table S17: *T1*-diagnostic and **spin-contamination values, $<S^2>$** for all the stationary points involved in the reaction of DTP with OH-radical calculated at the **CCSD(T)/aug-cc-pVTZ level of theory**.

Reactions	Species	*T1*-Diagnostic	$<S^2>$ values
Reactants	$CF_3CH_2CFCl_2$	0.0118	0.0
	OH	0.0099	0.7499
Reaction 1A	CR1A	0.0117	0.7499
	TS1A	0.0160	0.7497
	PC1A	0.0130	0.7499
	P1A	0.0133	0.7499
	H_2O	0.0100	0.0
Reaction 2A	CR2A	0.0118	0.7499
	TS2A	0.0159	0.7497
	PC2A	0.0130	0.7499
	P2A	0.0133	0.7499
Reaction 3A	CR3A	0.0117	0.7499
	TS3A	0.0191	0.7479
	PC3A	0.0141	0.7499
	P3A	0.0140	0.7499
	HOCl	0.0113	0.0
Reaction 4A	CR4A	0.0117	0.7499
	TS4A	0.0188	0.7480
	PC4A	0.0135	0.7499
	P4A	0.0139	0.7499

Table S18: *T1*-diagnostic and **spin-contamination values, $<S^2>$** for all the stationary points involved in the reaction of DTP with Cl-atom calculated at the **CCSD(T)/aug-cc-pVTZ level of theory**.

Reactions	Species	*T1*-Diagnostic	$<S^2>$ values
Reactants	$CF_3CH_2CFCl_2$	0.0118	0.0
	Cl	0.0066	0.7499
Reaction 1B	CR1B	0.0120	0.7499
	TS1B	0.0134	0.7495
	PC1B	0.0127	0.7499
	P1B	0.0132	0.7499
	HCl	0.0061	0.0
Reaction 2B	CR2B	0.0119	0.7488
	TS2B	0.0134	0.7496
	PC2B	0.0127	0.7499
	P2B	00133	0.7499
Reaction 3B	CR3B	0.0120	0.7499
	TS3B	0.0175	0.7481
	PC3B	0.0139	0.7499
	P3B	0.0140	0.7499
	Cl_2	0.0085	0.0
Reaction 4B	CR4B	0.0012	0.7499
	TS4B	0.0174	0.7482
	PC4B	0.0133	0.7499
	P4B	0.0130	0.7499

Table S19: Calculated Equilibrium constant (K_{eq}), unimolecular rate coefficient (k_{uni}) and overall rate coefficients (k_{1A}, k_{2A}, k_{3A}, k_{4A}) for the reaction channel **R1A, R2A, R3A**, and **R4A** in the 200-400 K temperature range at the **M06-2X level of theory**. Units of rate coefficients are in cm^3 $molecule^{-1}$ s^{-1}.

k1A			
Temperature	K_{eq}	k_2	k_{1A}
200	0.143	4.00×10^{7}	9.49×10^{-15}
220	0.0514	6.50×10^{7}	5.55×10^{-15}
240	0.022	1.00×10^{8}	3.65×10^{-15}
260	0.0108	1.60×10^{8}	2.87×10^{-15}
280	0.0059	2.50×10^{8}	2.46×10^{-15}
298	0.0037	3.60×10^{8}	2.22×10^{-15}
300	0.0035	3.70×10^{8}	2.18×10^{-15}
320	0.0023	5.50×10^{8}	2.06×10^{-15}
340	0.0015	8.00×10^{8}	2.03×10^{-15}
360	0.0011	1.10×10^{9}	1.97×10^{-15}
380	0.0008	1.60×10^{9}	2.12×10^{-15}
400	0.0006	2.10×10^{9}	2.13×10^{-15}

k_{2A} ***(R2A)***			
Temperature	K_{eq}	k_2	k_{2A}
200	0.1430	4.00×10^{7}	9.49×10^{-15}
220	0.0486	6.30×10^{7}	5.08×10^{-15}
240	0.0200	9.80×10^{7}	3.25×10^{-15}
260	0.0095	1.50×10^{8}	2.35×10^{-15}
280	0.0050	2.30×10^{8}	1.91×10^{-15}
298	0.0031	3.30×10^{8}	1.67×10^{-15}
300	0.0029	3.40×10^{8}	1.64×10^{-15}
320	0.0018	5.10×10^{8}	1.53×10^{-15}
340	0.0012	7.30×10^{8}	1.44×10^{-15}
360	0.0008	1.00×10^{9}	1.38×10^{-15}
380	0.0006	1.40×10^{9}	1.40×10^{-15}
400	0.0005	1.90×10^{9}	1.43×10^{-15}

k_{3A} (R3A)			
Temperature	K_{eq}	k_2	k_{3A}
200	0.1920	1.20×10^{-16}	3.83×10^{-38}
220	0.06870	5.50×10^{-14}	6.27×10^{-36}
240	0.02930	9.00×10^{-12}	4.38×10^{-34}
260	0.01430	6.80×10^{-10}	1.61×10^{-32}
280	0.00782	2.70×10^{-8}	3.51×10^{-31}
298	0.00488	5.10×10^{-7}	4.13×10^{-30}
300	0.00465	6.80×10^{-7}	5.25×10^{-30}
320	0.00296	1.10×10^{-5}	5.41×10^{-29}
340	0.00200	1.30×10^{-4}	4.32×10^{-28}
360	0.00142	1.20×10^{-3}	2.83×10^{-27}
380	0.00104	8.80×10^{-3}	1.52×10^{-26}
400	0.00080	5.20×10^{-2}	6.87×10^{-26}

k_{4A} (R4A)			
Temperature	K_{eq}	k_2	k_{4A}
200	0.1520	1.80×10^{-19}	4.54×10^{-41}
220	0.0542	1.30×10^{-16}	1.17×10^{-38}
240	0.0231	3.40×10^{-14}	1.30×10^{-36}
260	0.0113	3.80×10^{-12}	7.13×10^{-35}
280	0.0061	2.10×10^{-10}	2.13×10^{-33}
298	0.0038	5.10×10^{-9}	3.23×10^{-32}
300	0.0036	6.90×10^{-9}	4.16×10^{-32}
320	0.0023	1.50×10^{-7}	5.75×10^{-31}
340	0.0016	2.20×10^{-6}	5.66×10^{-30}
360	0.0011	2.40×10^{-5}	4.38×10^{-29}
380	0.0008	2.00×10^{-4}	2.68×10^{-28}
400	0.0006	1.40×10^{-3}	1.43×10^{-27}

Table S20: Calculated overall rate coefficients for the reaction of $CCl_2FCH_2CF_3$ with OH-radical in the 200-400 K temperature range at the **M06-2X level of theory**. Units are in cm^3 $molecule^{-1}$ s^{-1}.

Temperature	k_{1A}	k_{2A}	k_{3A}	k_{4A}	k_{over}
200	9.49×10^{-15}	9.49×10^{-15}	3.83×10^{-38}	4.54×10^{-41}	1.89×10^{-14}
220	5.55×10^{-15}	5.08×10^{-15}	6.27×10^{-36}	1.17×10^{-38}	1.06×10^{-14}
240	3.65×10^{-15}	3.25×10^{-15}	4.38×10^{-34}	1.30×10^{-36}	6.91×10^{-15}
260	2.87×10^{-15}	2.35×10^{-15}	1.61×10^{-32}	7.13×10^{-35}	5.22×10^{-15}
280	2.46×10^{-15}	1.91×10^{-15}	3.51×10^{-31}	2.13×10^{-33}	4.37×10^{-15}
298	2.22×10^{-15}	1.67×10^{-15}	4.13×10^{-30}	3.23×10^{-32}	3.88×10^{-15}
300	2.18×10^{-15}	1.64×10^{-15}	5.25×10^{-30}	4.16×10^{-32}	3.81×10^{-15}
320	2.06×10^{-15}	1.53×10^{-15}	5.41×10^{-29}	5.75×10^{-31}	3.59×10^{-15}
340	2.03×10^{-15}	1.44×10^{-15}	4.32×10^{-28}	5.66×10^{-30}	3.47×10^{-15}
360	1.97×10^{-15}	1.38×10^{-15}	2.83×10^{-27}	4.38×10^{-29}	3.35×10^{-15}
380	2.13×10^{-15}	1.40×10^{-15}	1.52×10^{-26}	2.68×10^{-28}	3.52×10^{-15}
400	2.13×10^{-15}	1.43×10^{-15}	6.87×10^{-26}	1.43×10^{-27}	3.55×10^{-15}

Table S21: Calculated Equilibrium constant (K_{eq}), unimolecular rate coefficient (k_{uni}) and overall rate coefficients (k_{1B}, k_{2B}, k_{3B}, k_{4B}) for the reaction channel **R1B, R2B, R3B**, and **R4B** in the 200-400 K temperature range at the **M06-2X level of theory**. Units of rate coefficients are in cm^3 $molecule^{-1}$ s^{-1}.

k_{1B} (R1B)			
Temperature	K_{eq}	k_2	k_{1B}
200	0.468	1.00×10^{3}	7.77×10^{-19}
220	0.198	5.20×10^{3}	1.71×10^{-18}
240	0.097	2.20×10^{4}	3.55×10^{-18}
260	0.053	7.90×10^{4}	6.99×10^{-18}
280	0.032	2.40×10^{5}	1.28×10^{-17}
298	0.021	6.10×10^{5}	2.17×10^{-17}
300	0.021	6.70×10^{5}	2.29×10^{-17}
320	0.014	1.60×10^{6}	3.72×10^{-17}
340	0.010	3.60×10^{6}	5.98×10^{-17}
360	0.007	7.50×10^{6}	9.27×10^{-17}
380	0.006	1.50×10^{7}	1.42×10^{-16}
400	0.005	2.60×10^{7}	1.94×10^{-16}

k_{2B} (R2B)			
Temperature	K_{eq}	k_2	k_{2B}
200	0.2360	1.90×10^{2}	7.45×10^{-20}
220	0.0952	1.20×10^{3}	1.90×10^{-19}
240	0.0448	5.90×10^{3}	4.39×10^{-19}
260	0.0238	2.50×10^{4}	9.88×10^{-19}
280	0.0138	8.80×10^{4}	2.02×10^{-18}
298	0.0091	2.50×10^{5}	3.76×10^{-18}
300	0.0087	2.70×10^{5}	3.89×10^{-18}
320	0.0058	7.50×10^{5}	7.20×10^{-18}
340	0.0040	1.80×10^{6}	1.21×10^{-17}
360	0.0029	4.20×10^{6}	2.06×10^{-17}
380	0.0022	8.80×10^{6}	3.26×10^{-17}
400	0.0017	1.70×10^{7}	4.88×10^{-17}

k_{3B} (R3B)			
Temperature	K_{eq}	k_2	k_{3B}
200	0.045	7.20×10^{-14}	5.34×10^{-36}
220	0.190	1.80×10^{-11}	5.68×10^{-33}
240	0.094	1.80×10^{-9}	2.80×10^{-31}
260	0.052	9.20×10^{-8}	7.87×10^{-30}
280	0.031	2.60×10^{-6}	1.34×10^{-28}
298	0.021	3.80×10^{-5}	1.31×10^{-27}
300	0.020	4.80×10^{-5}	1.59×10^{-27}
320	0.014	6.20×10^{-4}	1.40×10^{-26}
340	0.010	5.90×10^{-3}	9.56×10^{-26}
360	0.007	4.20×10^{-2}	5.06×10^{-25}
380	0.006	2.60×10^{-1}	2.41×10^{-24}
400	0.044	1.30×10^{0}	9.52×10^{-23}

k_{4B} (R4B)			
Temperature	K_{eq}	k_2	k_{4B}
200	0.2740	1.50×10^{-14}	6.82×10^{-36}
220	0.1100	4.50×10^{-12}	8.22×10^{-34}
240	0.0519	5.20×10^{-10}	4.48×10^{-32}
260	0.0275	2.90×10^{-8}	1.32×10^{-30}
280	0.0160	9.10×10^{-7}	2.42×10^{-29}
298	0.0104	1.40×10^{-5}	2.42×10^{-28}
300	0.0100	1.80×10^{-5}	2.99×10^{-28}
320	0.0067	2.50×10^{-4}	2.76×10^{-27}
340	0.0047	2.60×10^{-3}	2.01×10^{-26}
360	0.0034	2.00×10^{-2}	1.13×10^{-25}
380	0.0026	1.30×10^{-1}	5.53×10^{-25}
400	0.0019	6.80×10^{-1}	2.25×10^{-24}

Table S22: Calculated overall rate coefficients for the reaction of $CCl_2FCH_2CF_3$ with Cl-atom in the 200-400 K temperature range at the **M06-2X level of theory**. Units are in cm^3 $molecule^{-1}$ s^{-1}.

Temperature	k_{1B}	k_{2B}	k_{3B}	k_{4B}	$k_{o,Cl}$
200	7.77×10^{-19}	7.45×10^{-20}	5.34×10^{-36}	6.82×10^{-36}	8.52×10^{-19}
220	1.71×10^{-18}	1.90×10^{-19}	5.68×10^{-33}	8.22×10^{-34}	1.90×10^{-18}
240	3.55×10^{-18}	4.39×10^{-19}	2.80×10^{-31}	4.48×10^{-32}	3.99×10^{-18}
260	6.99×10^{-18}	9.88×10^{-19}	7.87×10^{-30}	1.32×10^{-30}	7.98×10^{-18}
280	1.28×10^{-17}	2.02×10^{-18}	1.34×10^{-28}	2.42×10^{-29}	1.48×10^{-17}
298	2.17×10^{-17}	3.76×10^{-18}	1.31×10^{-27}	2.42×10^{-28}	2.54×10^{-17}
300	2.29×10^{-17}	3.89×10^{-18}	1.59×10^{-27}	2.99×10^{-28}	2.68×10^{-17}
320	3.72×10^{-17}	7.20×10^{-18}	1.40×10^{-26}	2.76×10^{-27}	4.44×10^{-17}
340	5.98×10^{-17}	1.21×10^{-17}	9.56×10^{-26}	2.01×10^{-26}	7.19×10^{-17}
360	9.27×10^{-17}	2.06×10^{-17}	5.06×10^{-25}	1.13×10^{-25}	1.13×10^{-16}
380	1.42×10^{-16}	3.26×10^{-17}	2.41×10^{-24}	5.53×10^{-25}	1.75×10^{-16}
400	1.94×10^{-16}	4.88×10^{-17}	9.52×10^{-23}	2.25×10^{-24}	2.43×10^{-16}

Notes 2: Eckart Unsymmetrical Potential Barrier.

The analytic form of the Eckart unsymmetrical potential barrier was proposed by Eckart and can model a variety of reasonable shapes. It calculates the probability of transmission p(E) through the corresponding 1D-barrier at energy E. The p(E) is given by [1,2]

$$p(E) = 1 - \left[\frac{\cosh[2\pi(\alpha-\beta)]+\cosh[2\pi\delta]}{\cosh[2\pi(\alpha+\beta)]+\cosh[2\pi\delta]}\right]$$

$$\alpha = \frac{1}{2\sqrt{C}}\sqrt{E}, \beta = \frac{1}{2\sqrt{C}}\sqrt{E-A}, \delta = \frac{1}{2\sqrt{C}}\sqrt{B-C}$$

Where, $A = \Delta H_f - \Delta H_r, B = (\sqrt{\Delta H_f} - \sqrt{\Delta H_r})^2$ and $C = (h\, Im(v^{\ddagger}))^2[\frac{B^3}{(A^2-B^2)}]^2$

The constants (A, B) determine the overall shape of the Eckart barrier are linked to the zero-point energy barriers in the reverse and forward directions. The Eckart tunnelling corrections $[\chi(\mathrm{T})]$ is obtained numerically integrating p(E) over Boltzmann distribution of energies

$$\chi(\mathrm{T}) = \frac{e^{\frac{\Delta H_f}{k_b T}}}{k_b T}\int_0^{\infty} p(E)e^{\frac{-E}{k_b T}}dE$$

References

1. C. Eckart, *Phys. Rev.* 1930, **35**, 1303– 1309.
2. H. S. Johnston and J. Heicklen, *J. Phys. Chem.*, 1962, **66**, 532– 533.

Table S23: Vibrational frequencies which are treated as hindered rotors for the species involved in the dominant reaction channels (R1A, R2A, R1B, and R2B) calculated at the M06-2X/cc-pVTZ level of theory. Units are in cm^{-1}.

Reactant ($CF_3CH_2CFCl_2$)	**R1A**			**R2A**		
	CR1A	**TS1A**	**PC1A**	**CR2A**	**TS2A**	**PC2A**
30.37	66.84	17.20	27.45	28.92	33.68	25.62
123.34		135.51	93.20			49.94
						73.28

R1B			**R2B**		
CR1B	**TS1B**	**PC1B**	**CR2B**	**TS2B**	**PC2B**
16.87	21.64	27.05	35.43	30.83	38.09
35.08	45.56	39.01	135.36	100.82	56.11
126.14					

We have computed the partition functions using the hindered rotor (HR) approximation. The HR calculations for determining the partition function have been carried out using the Gaussian 16 software [1]. We used the keyword ***freq = hinderedrotor*** or ***freq = readhinderedrotor*** with additional keywords depending upon the structure of the species. The additional keywords have been added using the Gaussian 16 online manual. A few lower frequencies of the species involved in each reaction channels are treated as hindered rotors as shown in Table S23.

Notes 4: Hindered Rotor (HR) Approximation

The partition function is the bridge between the microscopic quantum mechanical properties of a molecule and its macroscopic thermodynamic properties, defined in the canonical ensemble as [2,3]

$$q = \sum_j e^{\frac{-E_j}{k_B T}} \tag{S1}$$

Where E_j is the energy of the j^{th} state. Then, the total partition function is given by [4]

$$q = q_{trans} q_{rot} q_{vib} q_{elec} \tag{S2}$$

Where q_{trans} is the translational partition function, q_{rot} is the rotational partition function, q_{vib} is the vibrational partition function, and q_{elec} is the electronic partition function.

Previous studies [2,4,5] have revealed that the harmonic oscillator (HO) approximation effectively describes high-frequency vibrational modes. However, HO approximation is often inadequate for low-frequency vibrational modes, primarily resulting from the torsional rotation of the single bonds [6,7]. Such type of modes undergo hindered rotation. A simple approach for computing vibrational partition functions involving torsional rotation assumes that the normal modes are decoupled. The HO approximation is then utilised for the non-torsional modes, while the HR approximation is applied to the torsional modes. Thus, the vibrational partition function $\left(q_{vib}^{HO-HR}\right)$ can be written as [2]

$$q_{vib}^{HO-HR} = q_{HO} q_{HR} \tag{S3}$$

$$q_{HO} = \prod_{i=1}^{F} \frac{e^{\left(-\frac{h\nu_i}{2k_B T}\right)}}{1-e^{\left(-\frac{h\nu_i}{k_B T}\right)}} \tag{S4}$$

Where q^{HO} and q^{HR} are the partition functions of the quantum harmonic oscillator and hindered rotor, respectively; F is the number of non-torsional modes, and ν_i is the vibrational frequency of the i^{th} non-torsional mode.

Computing hindered rotor partition function (q_{HR})

One of the most widely used methods for dealing with torsions was derived by Pitzer and Gwinn [8] in the 1940s, who solved the Schrödinger equation numerically for one dimensional hindered rotor (1D-HR)

$$-\frac{\hbar^2}{2I_r}\frac{d^2\Psi_{HR}}{d\varphi^2} + V\Psi_{HR} = E\Psi_{HR} \tag{S5}$$

Where $\Psi_{HR}, \varphi, E,$ and I_r are the wave function of the HR, torsional angle, energy, and reduced moment of Inertia, respectively. $\hbar$ is the Dirac constant ($\frac{h}{2\pi}$), and V is the torsional potential. V is further expressed as

$$V = \frac{V_o}{2}(1 - \cos M\varphi) \tag{S6}$$

Where V_o is the torsional barrier, M is the total minima along coordinate (periodicity) in the range (0 – 2π). Eqn. (S5) can be transformed into Mathieu's equation [9,10] and solved to obtain energy eigenvalues that give the partition function and other thermodynamics parameters.

Pitzer and Gwinn [11] additionally suggested an analytical expression (PG model, q_{HR}^{PG}) of the HR partition function by correcting the classical partition function, q_{class}, with the ratio of the quantum and classical HO partition function, q_{HO} and q_{CHO}, respectively.

$$q_{HR}^{PG} = q_{class}(\frac{q_{HO}}{q_{CHO}}) \tag{S7}$$

$$q_{CHO} = \frac{k_B T}{h\upsilon} \tag{S8}$$

$$q_{class} = \frac{(2\pi k_B T)^{1/2}}{h}\int_0^{2\pi/M} I_r^{1/2} e^{-\frac{V_0}{2RT}(1-cosM\varphi)}\, d\varphi \tag{S9}$$

Where υ is the torsional frequency, h is Planck's constant, and R is the gas constant. When symmetric HR is considered, I_r remains constant. Thus, solving eqn. (S9), we get

$$q_{class} = q_{FR} e^{-\frac{V_0}{2RT}} I_0(V_0/RT) \tag{S10}$$

Where I_0 is the modified Bessel function of the first type of zeroth-order [12] and I_r is the moment of inertia that can be obtained from the exact method of PG. Again, the total q_{FR} is the free rotor partition function given by

$$q_{FR} = \frac{(8\pi^3 I_{eff} k_B T)^{1/2}}{Mh} \tag{S11}$$

Where $I_{eff} = I_{R_1} I_{R_2}/(I_{R_1} + I_{R_2})$, R_1, and R_2 are two fragments rotating relative to each other through the torsional axis, and I_{R_1} and I_{R_2} are their respective moments of inertia.

Subsequently, Hui-yun [13] developed the Modified Pitzer-Gwinn (MPG) method, based on the PG approach, to achieve high accuracy at elevated temperatures. For high temperatures, the

partition function by MPG method (q_{HR}^{MPG}) provides accurate values compared to q_{HR}^{PG}, but it failed when $T \rightarrow 0$ [2].

To overcome this failure, Truhlar introduced a new method (correction to the PG model, q_{HR}^{T91}) for the calculation of the partition function that works at low temperatures. Thus, q_{HR}^{T91} can be written as [2,4,13]

$$q_{HR}^{T91} = q_{HO} \tanh(\frac{q_{FR}}{q_{CHO}}) \quad \text{(S12)}$$

Later, more corrections to the PG model were proposed by McClurg, Flagen, and Goddard [14-16] (MFG) and Ayala and Schlegel [12] (AS) that adjust the partition function by introducing a multiplicative factor.

The MFG scheme (q_{HR}^{MFG}) employs the Padé approximation [15] to correct the overestimation of the zero-point energy (ZPE) [16].

$$q_{HR}^{MFG} = q_{HR}^{PG} \Delta E^{MFG} \quad \text{(S13)}$$

Where $\Delta E^{MFG} = h^2 v^2/(2hv + 16V_0)$ is the difference between the ZPE of the quantum HO and the HR.

Again, Ayala and Schlegel's approach (AS) [6] aimed to achieve better results for small torsional barriers and high temperatures using a polynomial factor.

$$q_{HR}^{AS} = q_{HR}^{PG} \left(\frac{1+P_2 e^{-V_0/2RT}}{1+P_1 e^{-V_0/2RT}}\right) \quad \text{(S14)}$$

Where P_1 and P_2 are fifth-order polynomial functions of $x = 1/q_{FR}$ and $y = V_0/RT$, and the torsional barrier is

$$V_0 = \frac{8\pi^2 v^2 I_r N_A}{M^2} \quad \text{(S15)}$$

Where N_A is the Avogadro's number.

In Gaussian 16 software, the Ayala and Schlegel approach (q_{HR}^{AS}), which is the modification of the PG, T91, and MFG approach, is implemented for the calculations of the hindered rotor partition functions.

References

1. M. J. Frisch, G. W. Trucks, H. B. Schlegel, G. E. Scuseria, M. A. Robb, J. R. Cheeseman, G. Scalmani, V. Barone, G. A. Petersson, H. Nakatsuji, X. Li, M. Caricato, A. V. Marenich, J. Bloino, B. G. Janesko, R. Gomperts, B. Mennucci, H. P. Hratchian, J. V. Ortiz, A. F. Izmaylov, J. L. Sonnenberg, D. WilliamsYoung, F. Ding, F. Lipparini, F. Egidi, J. Goings, B. Peng, A. Petrone, T. Henderson, D. Ranasinghe, V. G. Zakrzewski, J. Gao, N. Rega, G. Zheng, W. Liang, M. Hada, M. Ehara, K. Toyota, R. Fukuda, J. Hasegawa, M. Ishida, T. Nakajima, Y. Honda, O. Kitao, H. Nakai, T. Vreven, K. Throssell, J. A. Montgomery, Jr., J. E. Peralta, F. Ogliaro, M. J. Bearpark, J. J. Heyd, E. N. Brothers, K. N. Kudin, V. N. Staroverov, T. A. Keith, R. Kobayashi, J. Normand, K. Raghavachari, A. P. Rendell, J. C. Burant, S. S. Iyengar, J. Tomasi, M. Cossi, J. M. Millam, M. Klene, C. Adamo, R. Cammi, J. W. Ochterski, R. L. Martin, K. Morokuma, O. Farkas, J. B. Foresman and D. J. Fox, *Gaussian 16 Revision C.01*, 2016, Gaussian Inc. Wallingford CT.
2. E. Dzib and G. Merino, *Wiley Interdiscip. Rev. Comput. Mol. Sci.*, 2022, **12**, e1583 (1–25).
3. E. Dzib, J. L. Cabellos, F. O. Chi, S. Pan, A. Galeno and G. Merino, *Int. J. Quantum Chem.*, 2022, **119**, e25686 (1–10).
4. C. N. Banwell, *Fundamentals of Molecular* Spectroscopy, McGrawhill, 1966.
5. C. Cervinka, M. Fulem, and K. Ruzicka, *J. Chem. Eng. Data.*, 2012, **57**, 227–232.
6. P. Y. Ayala and H. B. Schlegel, *J. Chem. Phys.*, 1998, **108**, 2314–2325.
7. Y. Gao, T. He, X. Li, and X. You, *Phys. Chem. Chem. Phys.*, 2019, **21**, 1928–1936.
8. K. S. Pitzer and W. D. Gwinn, *J. Chem. Phys.*, 1946, **14**, 239–243.
9. G. B. Arfken and H. J. Weber, *Mathematical methods for Physicist*, 6th Edition, New York, NY, *Elsevier*, 2005.
10. M. Gadella, H. Giacomini, L. P. Lara, *Appl. Math. Comput.*, 2015, **271**, 436–445.
11. K. S. Pitzer, and D. G. William, *J. Chem. Phys.*, 1942, **10**, 428–440.
12. P. Hui-Yun, *J. Chem. Phys.*, 1987, **87**, 4846–4848.
13. D. G. Truhlar, *J. Comput. Chem.* 1991, **12**, 266–270.
14. R. B. McClurg, R. C. Flagan, and W. A. Goddard III, *J. Chem. Phys.*, 1997, **106**, 6675–6680.
15. R. B. McClurg, *J. Chem. Phys.*, 1998, **108**, 1748–1749.
16. R. B. McClurg, *J. Chem. Phys.*, 1999, **111**, 7163–7164.

Table S24: Calculated Eckart tunneling contributions (Γ_x, x = OH-1A, OH-2A, OH-3A, OH-4A) for all the four reaction channels (R1A, R2A, R3A, R4A) involved in the reaction of DTP with ˙OH in the temperature range of 200-400 K using Eyringpy Program code at the **M06-2X level of theory**.

Temperature	$\Gamma_{OH\text{-}1A}$	$\Gamma_{OH\text{-}2A}$	$\Gamma_{OH\text{-}3A}$	$\Gamma_{OH\text{-}4A}$
200	642	1011.7	1.3	1.3
220	200	297.7	1.3	1.3
240	81.3	115	1.2	1.2
260	40.3	54.5	1.2	1.2
280	23.2	30.2	1.2	1.1
298	15.5	19.5	1.1	1.1
300	14.9	18.8	1.1	1.1
320	10.5	12.8	1.1	1.1
340	7.8	9.4	1.1	1.1
360	6.2	7.2	1.1	1.1
380	5.1	5.8	1.1	1.1
400	4.3	4.9	1.1	1.1

Table S25: Calculated Eckart tunneling contributions (Γ_x, x = Cl-1B, Cl-2B, Cl-3B, Cl-4B) for all the four reaction channels (R1B, R2B, R3B, R4B) involved in the reaction of DTP with Cl-atom in the temperature range of 200-400 K using Eyringpy Program code at the **M06-2X level of theory**.

Temperature	$\Gamma_{\text{Cl-1B}}$	$\Gamma_{\text{Cl-2B}}$	$\Gamma_{\text{Cl-3B}}$	$\Gamma_{\text{Cl-4B}}$
200	12.3	20.1	1.1	1.2
220	7.2	10.4	1.1	1.2
240	5	6.6	1.1	1.1
260	3.8	4.7	1.1	1.1
280	3.1	3.7	1.1	1.1
298	2.7	3.1	1.1	1.1
300	2.6	3.1	1.1	1.1
320	2.3	2.7	1.1	1.1
340	2.1	2.4	1	1.1
360	1.9	2.1	1	1.1
380	1.8	2	1	1.1
400	1.7	1.8	1	1

Table S26: Branching ratio for the reaction of DTP with OH-radical in the 200-400 K temperature range.

Temperature	k_{1A}	k_{2A}	k_{3A}	k_{4A}
200	50.00	50.00	0.00	0.00
220	52.18	47.82	0.00	0.00
240	52.88	47.12	0.00	0.00
260	54.94	45.06	0.00	0.00
280	56.32	43.68	0.00	0.00
298	57.03	42.97	0.00	0.00
300	57.05	42.95	0.00	0.00
320	57.38	42.62	0.00	0.00
340	58.49	41.51	0.00	0.00
360	58.87	41.13	0.00	0.00
380	60.33	39.67	0.00	0.00
400	59.90	40.10	0.00	0.00

Table S27: **Branching ratio** for the reaction of DTP with Cl-atom in the 200-400 K temperature range.

Temperature	k_{1B}	k_{2B}	k_{3B}	k_{4B}
200	91.257	8.743	0.000	0.000
220	90.013	9.987	0.000	0.000
240	88.989	11.011	0.000	0.000
260	87.619	12.381	0.000	0.000
280	86.346	13.654	0.000	0.000
298	85.214	14.786	0.000	0.000
300	85.499	14.501	0.000	0.000
320	83.785	16.215	0.000	0.000
340	83.195	16.805	0.000	0.000
360	81.830	18.170	0.000	0.000
380	81.359	18.641	0.000	0.000
400	79.913	20.087	0.000	0.000

Notes 4: Radiative Efficiency Calculations.

Frequencies and their Intensities

The RE was calculated using the vibrational frequencies in the atmospheric window of 600-1600 cm^{-1} with respect to their corresponding intensities. The reactant is more effective if it absorb in this range [1,2]. Studies have revealed that even if this compound absorbs at other wavelength with strong absorption, the additional absorption will not contribute significantly to radiative forcing. All the frequencies are in cm^{-1}.

Table S28: Frequencies and Intensities of $CF_3CH_2CFCl_2$ calculated at the **M06-2X level of theory.**

Frequency	Intensities	RF per unit cross-section	Product
24.93	0.0274	0.0145	0.0003
120.20	1.5627	0.1740	0.2719
141.77	0.9981	0.2550	0.2545
230.54	0.0319	0.4200	0.0133
240.29	0.6811	0.5140	0.3500
304.58	0.5035	0.6780	0.3413
329.40	0.0147	0.7320	0.0107
385.13	0.5450	1.0600	0.5777
409.07	0.7238	1.2800	0.9264
468.78	3.3393	1.6500	5.5098
539.03	3.1031	2.2000	6.8268
550.24	1.3378	2.2100	2.9565
655.79	53.6284	0.0573	3.0729
706.63	53.1765	0.5100	27.1200
839.21	85.6440	3.2300	276.6301
890.83	51.7143	3.1000	160.3143
930.93	39.2821	2.9500	115.8821
1029.06	21.9293	1.4700	32.2360
1177.02	88.6612	1.5200	134.7650
1193.54	196.4481	1.5200	298.6011
1223.37	247.2957	1.1500	284.3900
1306.74	196.1598	0.2070	40.6050
1339.23	67.5589	0.2370	16.0114
1410.88	150.2967	0.0980	14.7290
1460.40	11.2224	0.0917	1.0290

RE= $(\sum v \times A_k) \times 1.66 \times 10^{-19} \times 10^{15}$ Wm^{-2} ppb^{-1}

=1405.3865 $\times$ $1.66 \times 10^{-19} \times 10^{15}$ Wm^{-2} ppb^{-1}

=0.2333 W m^{-2} ppb^{-1}

Also, $f(\tau)$ = 0.949

Again, a 10% increment in the RE on account of temperature adjustment in the stratosphere gives final RE = 0.246 W m^{-2} ppb^{-1}.

References

1. Ø. Hodnebrog, M. Etminan, J. Fuglestvedt, G. Marston, G. Myhre, C. Nielsen, K. P. Shine and T. J. Wallington, *Rev. Geophys.*, 2013, **51**, 300–378.
2. Ø. Hodnebrog, B. Aamaas, J. S. Fuglestvedt, G. Marston, G. Myhre, C. J. Nielsen, M. Sandstad, K. P. Shine and T. J. Wallington, *Rev. Geophys.*, 2020, **58**, e2019RG000691.